

First detection probability in quantum resetting via random projective measurements

Manas Kulkarni¹ and Satya N. Majumdar²

¹ International Centre for Theoretical Sciences, Tata Institute of Fundamental Research, Bengaluru – 560089, India

² LPTMS, CNRS, Univ. Paris-Sud, Université Paris-Saclay, 91405 Orsay, France

E-mail: manas.kulkarni@icts.res.in, satya.majumdar@u-psud.fr

Abstract.

We provide a general framework to compute the probability distribution $F_r(t)$ of the first detection time of a ‘state of interest’ in a generic quantum system subjected to random projective measurements. In our ‘quantum resetting’ protocol, resetting of a state is not implemented by an additional classical stochastic move, but rather by the random projective measurement. We then apply this general framework to Poissonian measurement protocol with a constant rate r and demonstrate that exact results for $F_r(t)$ can be obtained for a generic two level system. Interestingly, the result depends crucially on the detection schemes involved and we have studied two complementary schemes, where the state of interest either coincides or differs from the initial state. We show that $F_r(t)$ at short times vanishes universally as $F_r(t) \sim t^2$ as $t \rightarrow 0$ in the first scheme, while it approaches a constant as $t \rightarrow 0$ in the second scheme. The mean first detection time, as a function of the measurement rate r , also shows rather different behaviors in the two schemes. In the former, the mean detection time is a non-monotonic function of r with a single minimum at an optimal value r^* , while in the later, it is a monotonically decreasing function of r , signalling the absence of a finite optimal value. These general predictions for arbitrary two level systems are then verified via explicit computation in the Jaynes-Cummings model of light-matter interaction. We also generalise our results to non-Poissonian measurement protocols with a renewal structure where the intervals between successive independent measurements are distributed via a general distribution $p(\tau)$ and show that the short time behavior of $F_r(t) \sim p(0) t^2$ is universal as long as $p(0) \neq 0$. This universal t^2 law emerges from purely quantum dynamics that dominates at early times.

1. Introduction

Stochastic resetting in classical systems has emerged as a major area of research, both theoretically and experimentally, with a large number of applications across disciplines (for recent reviews see [1–3]). The basic idea behind stochastic resetting is as follows [4, 5]. Consider any system evolving under its own natural dynamics (which can be stochastic or deterministic). This natural dynamics is interrupted at random times and then the system restarts afresh from a ‘reset’ configuration. This reset configuration

is typically the initial configuration, but it can be any other fixed configuration [5]. The time interval τ between two successive resets is chosen independently from a distribution $p(\tau)$. For example, if $p(\tau) = r e^{-r\tau}$ (where the resetting occurs at a constant rate r) it is called the Poissonian resetting [1], while if reset occurs periodically/stroboscopically with a period T , it is referred to as ‘sharp restart’ [6, 7]. There are two principal outcomes of this resetting dynamics [4]: (i) resetting breaks detailed balance manifestly and drives the system into a nonequilibrium stationary state (NESS) and (ii) resetting typically makes the search of a fixed target by a random search process more efficient. For instance, the mean first-passage time to find a target in space by a diffusive searcher in any dimension gets minimized for a certain choice of the resetting rate r^* [4, 8]. These two paradigms have been tested in numerous theoretical models [6–22] and also in optical tweezer experiments in the recent past [23–25].

The same question can be asked also for a quantum system where the natural dynamics is deterministic, provided by the unitary evolution governed by the Schrödinger equation. The state of the system at time t is denoted by $|\psi(t)\rangle$. When this unitary evolution is interrupted at Poisson distributed random times and the state of the quantum system ‘restarts’ from its initial state, the density matrix of the system evolves into a NESS with nonzero off-diagonal elements [26] and this NESS has been investigated in various quantum systems [26–29]. However, the resetting of the quantum state to $|\Psi(0)\rangle$ is typically implemented ‘by hand’, i.e., by a classical stochastic move in these models. How this ‘quantum resetting’ can be actually implemented without using classical stochastic moves is an interesting question by itself. The other interesting issue is to define an analogue of the classical first passage probability in a quantum system. One way to implement this ‘quantum resetting’ is via standard projective measurement [30–32]. Suppose, we have a detector which tries to detect at ‘random times’ if the quantum system is in a particular ‘state of interest’ which we will denote by $|\psi_{\text{int}}\rangle$. If the outcome is ‘yes’, the state of the system immediately after the measurement attempt becomes $\hat{P}|\psi(t)\rangle$, where $\hat{P} = |\psi_{\text{int}}\rangle\langle\psi_{\text{int}}|$ denotes the projection operator into the state of interest $|\psi_{\text{int}}\rangle$. In contrast, if the outcome is ‘no’ the state of the system immediately after the measurement gets projected into $\hat{Q}|\psi(t)\rangle$, where $\hat{Q} = I - \hat{P}$ denotes the projection operator into the subspace of the Hilbert space that is complementary to the state of interest [33–54]. Then the system evolves unitarily till the next measurement attempt and so on. These measurements can occur stroboscopically with period T – this is the analogue of ‘sharp restart’ in classical systems. Similarly when the detection attempts take place at random epochs separated by an exponential distribution $p(\tau) = r e^{-r\tau}$, it is the analogue of Poissonian resetting in classical systems. Note that here the ‘quantum restart’ is not implemented by hand using classical moves, but rather the projective measurement itself does the job of resetting to a new state after every measurement attempt.

This projective measurement protocols also provide a natural analogue of the classical first passage probability, namely the first detection probability. For example, if the outcomes of successive measurements are $\{\text{no}, \text{no}, \dots, \text{no}, \text{yes}\}$, then when ‘yes’

appears for the first time, we say that the state is detected at that time. Clearly this first detection time is a random variable if the measurement times are also random and its probability distribution function (PDF) is the first detection probability [33–42, 48, 55–58]. Its first moment, namely the mean first detection time is thus a natural analogue of the mean first passage time in classical systems. The resetting rate in these quantum systems is just the rate of detection attempts, i.e., the rate of measurement. Note that this ‘quantum resetting’ via projective measurements is also different from the effective stochastic resetting dynamics exhibited by non-Hermitian quasiparticles describing the growth of entanglement in a class of quantum systems coupled to a measurement device [59].

Thus, in this paper, by ‘quantum resetting’ we simply mean projective measurements only and do not invoke any additional ‘classical restart’ moves by hand. We ask a simple and natural question: as in classical resetting systems, is there an optimal resetting rate, i.e., an optimal rate of measurement, that minimizes the mean first detection time in quantum resettings via projective measurements only? The existence of this optimal rate has been investigated recently in various quantum models, but usually in the presence of an additional ‘classical restart’ move [52, 53]. Here our goal is to investigate this optimal resetting rate in quantum systems subject only to random projective measurements via the Poissonian measurement protocol with rate r . We first provide a general framework to compute the first detection probability $F_r(t)$ in a quantum system with Poissonian protocol, and in particular, focus on generic two-level systems where explicit results can be obtained. We study two different detection schemes depending on whether the state of interest is different or identical to the initial state. We show the statistics of the first detection time is rather different in the two schemes. For instance, $F_r(t)$ at short times vanishes universally as $F_r(t) \sim t^2$ as $t \rightarrow 0$ in the first scheme, while it approaches a constant as $t \rightarrow 0$ in the second scheme. The mean first detection time, as a function of the measurement rate r , also shows rather different behaviors in the two schemes. In the first scheme, the mean first detection time exhibits a unique minimum as a function of r , thus confirming the existence of an optimal measurement rate in this quantum setting. In contrast, for the second scheme, we show that the mean first detection time is a monotonically decreasing function of r , showing that there is no finite optimal measurement rate. This last fact in scheme 2 was also noticed in Refs. [56, 57]—where scheme 2 is usually referred to as the ‘return’ problem of a quantum state to itself.

We then focus on a specific two level system, the Jaynes-Cummings (JC) model which is a prototypical model mimicking light-matter interaction [60–63]. The JC model can be effectively mapped to a two-level system for a given fixed excitation sector. The JC model subjected to ‘classical stochastic resetting’ (and not projective measurement) has been studied very recently and certain observables such as the fidelity etc. have been computed [51]. In this paper, we show that the integrable structure of the JC model allows us to compute explicitly the full PDF of the first detection time under projective Poissonian measurement protocol. This exact solution is useful since we can then test

and verify all our general predictions valid for arbitrary two level systems. Moreover, from the exact solution of the JC model we show that there exists another time scale $t_m(r)$ characterizing the late time exponential decay of the PDF of the first detection time. This time scale $t_m(r)$ is different from the standard mean first detection time which is just the first moment of the PDF. Physically, this time scale $t_m(r)$ represents the maximal waiting time to detect the state of interest beyond which there is no detection almost surely. Our exact calculation shows that this maximal time scale $t_m(r)$ in the JC model is identical for both detection schemes mentioned above and does exhibit a single minimum at an optimal value r_m^* . Finally, our results for arbitrary two level systems are generalized to non-Poissonian measurement protocols where the measurement events are still uncorrelated, but the waiting time between successive measurements are distributed via a general $p(\tau)$, not necessarily exponential as in the Poissonian case. We show that the short time behavior of $F_r(t) \sim p(0)t^2$ is universal as long as $p(0) \neq 0$.

The rest of the paper is organised as follows: In Sec. 2, we discuss the first detection probability and its cumulative distribution, which we call survival probability, when the system is subjected to unitary evolution and projective measurements at random times. This is done for a generic Hamiltonian and a generic random measurement protocol. In Sec. 3, assuming still a generic Hamiltonian, we discuss the Poissonian measurement protocol where a measurement is attempted at random continuous times with rate r and we provide a general framework to compute the PDF of the first detection time. In Sec. 4, we focus on a generic two-level system under Poissonian protocol where more explicit results can be obtained. We discuss two different detection schemes : (i) when the state of interest differs from the initial state and (ii) when they are identical. For a generic two level Hamiltonian, we derive the exact Laplace transform of the PDF of the first detection time and also discuss the exact asymptotic behavior of the mean first detection time for small and large detection rate r . In Sec. 5, we derive explicitly the PDF of the first detection time in the Jaynes-Cummings model for both detection schemes. In Sec. 6. we provide a generalization of the non-Poissonian measurement protocol where the waiting time between independent measurements are drawn from a general $p(\tau)$. Sec. 7 contains a summary and an outlook. Some details of the calculations are relegated to the appendices.

2. The first detection probability: general formalism

Consider a general quantum system with Hamiltonian H , prepared in an initial state $|\psi(0)\rangle$. Without any external coupling to environment, the state of the system evolves unitarily and at time t , it is given by

$$|\psi(t)\rangle = e^{-iHt}|\psi(0)\rangle. \quad (1)$$

Any attempt to measure or detect the system in some state results in an interruption of the unitary evolution. Suppose, at time t , we make an attempt to detect if the system is in a specific state $|\psi_{\text{int}}\rangle$, where the subscript ‘int’ stands for ‘state of interest’.

Immediately after the measurement, the state of the system changes depending on the outcome of the detection attempt. This new post measurement state can be characterized naturally in terms of the pair of projection operators

$$\hat{P} = |\psi_{\text{int}}\rangle\langle\psi_{\text{int}}| \quad (2)$$

$$\hat{Q} = I - \hat{P} = I - |\psi_{\text{int}}\rangle\langle\psi_{\text{int}}|. \quad (3)$$

The operator \hat{Q} projects a state to the complementary subspace of $|\psi_{\text{int}}\rangle$. If the outcome of the measurement is a success, then the state of the system immediately after the measurement becomes $\hat{P}|\psi(t)\rangle$. In contrast, if the measurement is a failure, the state becomes $\hat{Q}|\psi(t)\rangle$. This is precisely the projective measurement. Following the measurement attempt, the system again evolves unitarily starting from $\hat{P}|\psi(t)\rangle$ or from $\hat{Q}|\psi(t)\rangle$, depending on the outcome of the first result, until another measurement is attempted at a future time. Thus, successive projective measurements are like successive ‘quantum resettings’ of the state of the system – resetting in this context simply means hitting the state with a projection operator which in this case could be either \hat{Q} or \hat{P} .

A question that arises naturally is: when is the first time t_r that the state of interest $|\psi_{\text{int}}\rangle$ will be detected if one keeps making measurements? Here we use the subscript r to denote ‘resetting’ in general. Obviously t_r depends on the details of the measurement protocol. In this paper, we will consider random measurements where attempts at detecting the state of interest occurs at random times T_1, T_2, T_3 etc; In that case, the first detection time t_r also becomes a random variable with a probability distribution function (PDF) denoted by $F_r(t) = \text{Prob.}[t_r = t]$. Our main goal in this paper is to compute $F_r(t)$ for a class of Hamiltonians H and some specific random measurement protocols.

This question concerning the first detection time in projective measurements has been addressed in a number of recent papers [37–41, 48, 56, 57]. Most of these papers addressed a stroboscopic measurement protocol where a measurement is attempted periodically with a fixed period T , with the exception of Refs. [48, 56, 57] where more general measurement protocols were discussed. Ref. [41, 56] developed a renewal formalism for general random measurement protocols to compute the first detection probability directly and used it to study a quantum random walk model [41, 48]. Below we present an alternative general formalism that is also adaptable to any measurement protocol. In our approach, it is more convenient to compute first the cumulative distribution of $F_r(t)$ (we call this survival probability below) and from it derive $F_r(t)$ by taking the derivative with respect to t , more in line with the approach used in Refs. [37, 38, 48].

As mentioned above, instead of computing the PDF of t_r directly, we find it more convenient to compute its cumulative distribution function (CDF) defined as

$$S_r(t) = \text{Prob.}[t_r \geq t] = \int_t^\infty F_r(t') dt'. \quad (4)$$

Thus, if we can compute $S_r(t)$, then the PDF of t_r follows simply from the derivative

$$F_r(t) = -\frac{dS_r(t)}{dt}. \quad (5)$$

The quantity $S_r(t)$ has a physical meaning: it is the probability that the state $|\psi_{\text{int}}\rangle$ is *not detected* up to time t under a given random measurement protocol. Since the process stops when the state of interest is detected for the first time, we will call $S_r(t)$, i.e., the probability of not being detected up to t , as the ‘survival probability’ up to t . An observable of much practical importance is the mean first detection time given by the first moment of $F_r(t)$, i.e.,

$$\bar{t}_r = \int_0^\infty t F_r(t) dt = \int_0^\infty S_r(t) dt, \quad (6)$$

where we used Eq. (5) and performed integration by parts with the initial condition $S_r(0) = 1$. Thus, knowing $S_r(t)$ allows us to compute easily the mean first detection time, as well as all higher moments of t_r .

The computation of $S_r(t)$ turns out to be simpler than that of $F_r(t)$ since one can break up $S_r(t)$ into a sum of terms representing the probability of 0, 1, 2, 3 etc. of failed detections up to t . For example, if there is no measurement event up to t , then the state of the system at time t is

$$|\psi_0(t)\rangle = e^{-iHt} |\psi(0)\rangle. \quad (7)$$

The subscript ‘0’ in $|\psi_0(t)\rangle$ stands for no measurement. Then the probability that the state $|\psi_{\text{int}}\rangle$ is not detected up to t is trivially

$$S_r(0, t) = \langle \psi_0(t) | \psi_0(t) \rangle = \langle \psi(0) | \psi(0) \rangle = 1, \quad (8)$$

where we assume that the initial state $|\psi(0)\rangle$ is normalized to unity. Here $S_r(0, t)$ denotes the survival probability up to t , conditioned on having no measurement prior to t . Now, suppose we make the first measurement at some time τ_1 , resulting in a failure. Then the state of the system immediately after this first failed detection is

$$|\psi_1(\tau_1)\rangle = \hat{Q} e^{-iH\tau_1} |\psi(0)\rangle. \quad (9)$$

The subscript ‘1’ denotes one measurement resulting in a failed detection. At any subsequent time $t \geq \tau_1$, if there are no measurement attempts in the interval $[\tau_1, t - \tau_1]$, the state of the system is given by

$$|\psi_1(t)\rangle = e^{-iH(t-\tau_1)} \hat{Q} e^{-iH\tau_1} |\psi(0)\rangle, \quad t \geq \tau_1. \quad (10)$$

In this case, the survival probability $S_r(1, t|\tau_1)$ up to t , conditioned on having one failed detection at $\tau_1 < t$, is simply

$$S_r(1, t|\tau_1) = \langle \psi_1(t) | \psi_1(t) \rangle = \langle \psi(0) | e^{iH\tau_1} \hat{Q}^\dagger \hat{Q} e^{-iH\tau_1} | \psi(0) \rangle. \quad (11)$$

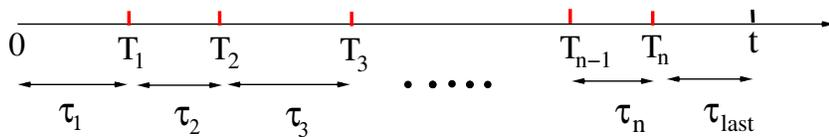


Figure 1. A schematic representation of a configuration of the random measurement protocol with n measurements taking place till time t at random epochs $T_1, T_2, T_3, \dots, T_n$. The interval between successive measurements are denoted by $\tau_k = T_k - T_{k-1}$, with $k = 1, 2, \dots, n$. The last interval $\tau_{\text{last}} = t - T_n = t - \sum_{k=1}^n \tau_k$ is ‘measurement free’.

Using $\hat{Q}^\dagger \hat{Q} = \hat{Q}$ (since \hat{Q} is a projection operator), this simplifies to

$$S_r(1, t|\tau_1) \equiv S_r(1|\tau_1) = \langle \psi(0) | e^{iH\tau_1} \hat{Q} e^{-iH\tau_1} | \psi(0) \rangle. \quad (12)$$

Note that $S_r(1, t|\tau_1)$ does not depend on t explicitly, but only on τ_1 . Hence, we denote it by $S_r(1|\tau_1)$ in Eq. (12). Finally, let us remark that till the time of the first measurement at τ_1 , the norm of the state does not change from its initial value $\langle \psi(0) | \psi(0) \rangle = 1$. But at any subsequent time t after the first failed measurement at τ_1 , the norm $S_r(1, t|\tau_1)$ is less than unity. Thus every time a measurement takes place it reduces the norm of the state.

Now, consider the case when there are two failed measurements, respectively at $T_1 = \tau_1$ and $T_2 = \tau_1 + \tau_2$, prior to t . The state of the system at time $t \geq \tau_1 + \tau_2$ is then given by

$$|\psi_2(t)\rangle = e^{-iH(t-(\tau_1+\tau_2))} \hat{Q} e^{-iH\tau_2} \hat{Q} e^{-iH\tau_1} | \psi(0) \rangle. \quad (13)$$

The subscript 2 in $|\psi_2(t)\rangle$ indicates 2 measurements both resulting in failed detections. In this case, the survival probability $S_r(2, t|\tau_1, \tau_2)$ up to t , conditioned on having two failed detections respectively at τ_1 and $\tau_1 + \tau_2$, is simply

$$S_r(2, t|\tau_1, \tau_2) = \langle \psi_2(t) | \psi_2(t) \rangle = \langle \psi(0) | e^{iH\tau_1} \hat{Q}^\dagger e^{iH\tau_2} \hat{Q}^\dagger \hat{Q} e^{-iH\tau_2} \hat{Q} e^{-iH\tau_1} | \psi(0) \rangle. \quad (14)$$

Using $\hat{Q}^\dagger \hat{Q} = \hat{Q}$, this reduces to

$$S_r(2, t|\tau_1, \tau_2) \equiv S_r(2|\tau_1, \tau_2) = \langle \psi(0) | e^{iH\tau_1} \hat{Q}^\dagger e^{iH\tau_2} \hat{Q} e^{-iH\tau_2} \hat{Q} e^{-iH\tau_1} | \psi(0) \rangle. \quad (15)$$

As in the case $n = 1$, we note that $S_r(2, t|\tau_1, \tau_2)$ does not depend on t explicitly, hence we denote it by $S_r(2|\tau_1, \tau_2)$.

We can then easily generalise to the case when there are n measurements prior to t all resulting in failed detections of the state of interest $|\psi_{\text{int}}\rangle$, taking place at epochs $\{T_1 = \tau_1, T_2 = \tau_1 + \tau_2, T_3 = \tau_1 + \tau_2 + \tau_3, \dots, T_n = \sum_{k=1}^n \tau_k\}$. These measurement epochs are separated by time intervals $\{\tau_1, \tau_2, \tau_3, \dots, \tau_n\}$ [see Fig. (1)]. If there are $n > 0$ such failed attempts prior to t , then the state of the system at time $t > T_n$, conditioned on having $n > 0$ failed attempts prior to t , is given by

$$|\psi_n(t)\rangle = e^{-iH\tau_{\text{last}}} \prod_{k=1}^n \hat{Q} e^{-iH\tau_k} | \psi(0) \rangle, \quad (16)$$

where $\tau_{\text{last}} = t - T_n$ denotes the length of the ‘measurement free’ last interval before t [see Fig. (1)]. The survival probability up to t , conditioned on having $n > 0$ such failed attempts before t occurring at epochs separated by intervals $\{\tau_i\} \equiv \{\tau_1, \tau_2, \dots, \tau_n\}$, is then given by the norm $\langle \psi_n(t) | \psi_n(t) \rangle$. From Eq. (16), it is clear that upon taking the norm, the contribution from the last interval $e^{-iH\tau_{\text{last}}}$ disappears since it represents the free unitary evolution following the last measurement till t as shown in Fig. (1). Consequently the resulting survival probability $S_r(n, t | \{\tau_i\})$ becomes independent of the last interval τ_{last} and is given by

$$\begin{aligned} S_r(n, t | \{\tau_i\}) &= \langle \psi_n(t) | \psi_n(t) \rangle \\ &= \langle \psi(0) | \left[\prod_{k=1}^n e^{iH\tau_k} \hat{Q}^\dagger \right] \left[\prod_{m=1}^n \hat{Q} e^{-iH\tau_{n-m+1}} \right] | \psi(0) \rangle \\ &\equiv S_r(n | \{\tau_i\}). \end{aligned} \quad (17)$$

Recall that $\hat{Q}^\dagger = \hat{Q}$ given in Eq. (3). As in the case of $n = 1$ and $n = 2$, we note that $S_r(n, t | \{\tau_i\})$ in Eq. (17) does not depend on t explicitly, but only on the interval lengths $\{\tau_i\}$ that occur till the n -th measurement preceding t . Hence, we denote it simply by $S_r(n | \{\tau_i\})$ in Eq. (17). Note that the case $n = 0$ is a bit special since there is no measurement, and consequently no failed attempt and $S_r(0, t) = 1$ as in Eq. (8). However, for convenience, we can still use the general formula in Eq. (17) even for $n = 0$ provided the intervening operator between $\langle \psi(0) |$ and $| \psi(0) \rangle$ is identified with the identity operator I . Thus, with this convention, $S_r(n, t | \{\tau_i\})$ in Eq. (17) also includes the $n = 0$ case.

Any measurement configuration showing ‘no detection’ up to t is fully characterized by the number of measurements n that take place up to time t , as well as by the random time intervals $\{\tau_1, \tau_2, \dots, \tau_n\}$ between two successive measurements (all measurement events resulting in failed detections) in a given configuration, as shown in Fig. (1). Clearly, given t , both n and the intervals $\{\tau_i\} = \{\tau_1, \tau_2, \dots, \tau_n\}$ are random variables whose statistics depend on the precise nature of the random measurement protocol. Generically, let $P(n, \{\tau_i\} | t)$ denote the joint distribution of n and the set $\{\tau_i\}$, given a fixed time t . In that case, considering all possible random number of measurements and the associated intervals between successive measurements till t , the total survival probability up to time t can be expressed by the compact formula

$$S_r(t) = \sum_{n=0}^{\infty} \int_0^{\infty} d\tau_1 \cdots \int_0^{\infty} d\tau_n P(n, \{\tau_i\} | t) S_r(n | \{\tau_i\}), \quad (18)$$

where $S_r(n | \{\tau_i\})$ is given in Eq. (17). Note that in this formula, quantum operators and states appear only in $S_r(n | \{\tau_i\})$, but not in $P(n, \{\tau_i\} | t)$ which is a pure classical probability that characterizes the random measurement protocol. Thus the total survival probability $S_r(t)$ up to t involves a convolution of quantum and classical dynamics, the later being induced by the stochastic projective measurements.

Even though the formula in Eq. (18) is exact for a generic Hamiltonian and a generic measurement protocol, it is somewhat formal. Our goal in the next two sections is to

show that for Poissonian measurement protocol and for a generic two-level Hamiltonian, the formal expression in Eq. (18) simplifies enormously and consequently, the survival probability $S_r(t)$, or equivalently the first detection probability $F_r(t) = -dS_r(t)/dt$, can be computed explicitly.

3. Poissonian Measurement Protocol

In this section we focus on a specific random measurement protocol known as the Poissonian protocol, for which the joint probability density $P(n, \{\tau_i\}|t)$ can be written in a nice explicit form. Consequently, the result in Eq. (18) simplifies considerably and takes a compact form in the Laplace space conjugate to t .

In the Poissonian protocol, the measurements take place stochastically in continuous time with a constant rate r . More precisely, in a small time dt , a measurement takes place with probability $r dt$ and with the complementary probability $(1 - r dt)$ no measurement occurs. This measurement process is Markovian since the probability of a measurement at the instant t is independent of the history of the measurement process till t . The probability that an interval $[0, t]$ is ‘measurement free’ is then simply e^{-rt} . Furthermore, the intervals between successive measurements are statistically independent and the PDF of each interval τ_k is simply exponential, i.e., $p(\tau) = \text{Prob.}[\tau_k = \tau] = r e^{-r\tau}$. This follows from the fact that after the $(k - 1)$ -th measurement, one should have a measurement free interval of length τ (the probability of this event is $e^{-r\tau}$), followed by a measurement event at the end of this interval which occurs with probability $r d\tau$. Consequently, the PDF is $p(\tau) = \text{Prob.}[\tau_k = \tau] = r e^{-r\tau}$, which is normalized to unity. The Poissonian protocol appears quite naturally in classical stochastic resetting problems where r denotes the rate of resetting [1, 4, 5]. It also appears quite naturally in the run-and-tumble dynamics of active particles where r denotes the tumbling rate [64, 65].

We consider a ‘no detection’ measurement configuration up to a fixed t that is fully characterized by n (the number of measurements before t), the interval lengths $\{\tau_1, \tau_2, \tau_3, \dots, \tau_n\}$ between measurements, as depicted in Fig. (1). Given t and the set $\{\tau_1, \tau_2, \tau_3, \dots, \tau_n\}$, the length of the last interval gets fixed $\tau_{\text{last}} = t - \sum_{k=1}^n \tau_k$. Using the statistical independence of successive intervals, the joint probability density $P(n, \{\tau_i\}|t)$, given a fixed t , can then be written as the simple product [64, 65]

$$P(n, \{\tau_i\}|t) = \left[\prod_{k=1}^n r e^{-r\tau_k} \right] e^{-r(t - \sum_{k=1}^n \tau_k)}. \quad (19)$$

Note that, each of the τ_k ’s is distributed independently via the PDF $p(\tau) = r e^{-r\tau}$, but the last interval $\tau_{\text{last}} = t - \sum_{k=1}^n \tau_k$ is a bit apart. The statistical weight associated to it is $e^{-r\tau_{\text{last}}}$ without the additional multiplicative factor r unlike the intervals preceding it – this fact has been used and exploited in many recent contexts [64–67]. This is due to the fact that the last interval is measurement free and the probability for that is

just $e^{-r\tau_{\text{last}}}$. Thus the Poissonian protocol can be viewed as a classical continuous time renewal process with exponentially distributed intervals [68]

It is useful to check that the joint distribution in Eq. (19) is appropriately normalized to unity when one integrates over τ_k 's and sums over n . To check this, it is first convenient to express the joint PDF in Eq. (19) as an integral representation

$$P(n, \{\tau_i\}|t) = \int_0^\infty d\tau_{\text{last}} \left[\prod_{k=1}^n r e^{-r\tau_k} \right] e^{-r\tau_{\text{last}}} \delta(\tau_1 + \tau_2 + \dots + \tau_n + \tau_{\text{last}} - t). \quad (20)$$

The presence of the delta function naturally suggests to take the Laplace transform with respect to t . This gives, upon integrating over τ_{last} trivially,

$$\int_0^\infty P(n, \{\tau_i\}|t) e^{-st} dt = \frac{1}{r+s} \left[\prod_{k=1}^n r e^{-(r+s)\tau_k} \right]. \quad (21)$$

Now integrating over the set $\{\tau_i\}$ over $\tau_i \in [0, \infty]$, we get the Laplace transform of the marginal distribution $P(n|t)$ denoting the distribution of the number of measurements up to t ,

$$\int_0^\infty P(n|t) e^{-st} dt = \frac{r^n}{(r+s)^{n+1}}. \quad (22)$$

Inverting this Laplace transform gives the Poisson distribution

$$P(n|t) = e^{-rt} \frac{(rt)^n}{n!} \quad n = 0, 1, 2, \dots, \quad (23)$$

which justifies the name Poissonian protocol. Evidently $\sum_{n=0}^\infty P(n|t) = 1$, thus verifying that the joint PDF in Eq. (19) is correctly normalized to unity.

We now substitute the result Eq. (20) in the general formula for the survival probability in Eq. (18). This gives a rather long expression

$$S_r(t) = \sum_{n=0}^\infty \int_0^\infty d\tau_{\text{last}} e^{-r\tau_{\text{last}}} \left[\prod_{k=1}^n \int_0^\infty d\tau_k r e^{-r\tau_k} \right] S_r(n|\{\tau_i\}) \delta(\tau_1 + \dots + \tau_n + \tau_{\text{last}} - t). \quad (24)$$

Taking Laplace transform of Eq. (24) with respect to t and performing the integral over τ_{last} explicitly, one arrives at a slightly more compact expression

$$\tilde{S}_r(s) = \int_0^\infty dt e^{-st} S_r(t) = \frac{1}{r+s} \sum_{n=0}^\infty \left[\prod_{k=1}^n \int_0^\infty d\tau_k r e^{-(r+s)\tau_k} S_r(n|\{\tau_i\}) \right], \quad (25)$$

where $S_r(n|\{\tau_i\})$ is given in Eq. (17). Note that the first term in the summation corresponding to $n = 0$ is simply $1/(r+s)$. Hence it is useful to separate out the $n = 0$ term from the sum and write it as

$$\tilde{S}_r(s) = \int_0^\infty dt e^{-st} S_r(t) = \frac{1}{r+s} + \frac{1}{r+s} \sum_{n=1}^\infty \left[\prod_{k=1}^n \int_0^\infty d\tau_k r e^{-(r+s)\tau_k} S_r(n|\{\tau_i\}) \right]. \quad (26)$$

This result in Eq. (26) for the Poissonian protocol is valid for generic Hamiltonian H . However, Eq. (26) is still a bit formal because for a generic Hamiltonian H , it is not easy to compute explicitly $S_r(n|\{\tau_i\})$ in Eq. (17). In the next section, we show that for a two-level Hamiltonian H , one can compute $S_r(n|\{\tau_i\})$ explicitly. This leads to a simpler expression of the main result in Eq. (26).

4. Arbitrary two-level system with Poissonian measurement protocol

In the previous section, we derived the Laplace transform of the survival probability $S_r(t)$ up to time t [see Eq. (26)] for a system with a generic Hamiltonian H , subjected to Poissonian measurement protocol with rate r . As mentioned above, this formula [Eq. (26)] still contains the quantities $S_r(n|\{\tau_i\})$ which are hard to compute in practice for a general quantum Hamiltonian H with a large Hilbert space. In this section, we show that they can be computed in closed form for a general two-level system where the dimension of the Hilbert space is just two. The reason behind this is that the projection operator \hat{Q} involves only one state which makes the computation much simpler, as we illustrate below.

To be precise, we consider a general two-level Hamiltonian with two possible states in the Hilbert space, denoted respectively by $|\psi_+\rangle$ and $|\psi_-\rangle$. Without any loss of generality, we assume that the system is prepared at $t = 0$ in the $+$ state, i.e., $|\psi(0)\rangle = |\psi_+\rangle$. The complementary case when the system is initially in state $|\psi_-\rangle$ can be treated in a similar way. We will now consider two different schemes:

- Scheme 1: when the state of interest $|\psi_{\text{int}}\rangle$ differs from the initial state $|\psi_+\rangle$, i.e., when $|\psi_{\text{int}}\rangle = |\psi_-\rangle$.
- Scheme 2: when the state of interest coincides with the initial state, i.e., when $|\psi_{\text{int}}\rangle = |\psi_+\rangle$.

These two schemes are summarized in Table. 1. We remark that the second scheme has been studied recently for general two level systems subject to random measurement protocols using a different method [56,57]—where it is referred to as the ‘return problem’. Here we will show that our method allows to derive explicit results for both schemes under the same footing and also to compare the respective outcomes. We will show that the two schemes lead to very different results for the distribution of the first detection time and its moments. In particular, the short time behavior of the PDF of the first detection time as well as the mean detection time have drastically different behaviors in the two schemes.

We start by showing how the formula for $S_r(n|\{\tau_i\})$ in Eq. (17) simplifies for a two-level system such that the Laplace transform $\tilde{S}_r(s)$ in Eq. (26) can be expressed in terms of only two matrix elements. The key to the simplification for a two-level system lies in the fact that the projection operator $\hat{Q} = I - |\psi_{\text{int}}\rangle\langle\psi_{\text{int}}| = |\psi_c\rangle\langle\psi_c|$ involves a single state $|\psi_c\rangle$ which is complementary to $|\psi_{\text{int}}\rangle$ in either scheme. The subscript ‘c’ in $|\psi_c\rangle$ stands for ‘complementary’. Consequently $S_r(n|\{\tau_i\})$ etc. can be expressed very

	Initial State $ \psi(0)\rangle$	State of interest $ \psi_{\text{int}}\rangle$	$ \psi_c\rangle$	$f(\tau), g(\tau)$
1	$ \psi_+\rangle$	$ \psi_-\rangle$	$ \psi_+\rangle$	$f(\tau) = g(\tau)$
2	$ \psi_+\rangle$	$ \psi_+\rangle$	$ \psi_-\rangle$	$f(\tau) + g(\tau) = 1$

Table 1. The table demonstrates the detection schemes for a general two level system with two states $|\psi_+\rangle$ and $|\psi_-\rangle$ in its Hilbert space. The system is prepared initially in the + state, i.e., $|\psi(0)\rangle = |\psi_+\rangle$. There are two schemes depending on the state of interest $|\psi_{\text{int}}\rangle$. The scheme 1 corresponds to a situation when the initial state $|\psi(0)\rangle = |\psi_+\rangle$ is different from the state of interest $|\psi_{\text{int}}\rangle = |\psi_-\rangle$. The scheme 2 corresponds to the reverse situation when the initial state $|\psi(0)\rangle = |\psi_+\rangle$ is the same as the state of interest, i.e., $|\psi_{\text{int}}\rangle = |\psi_+\rangle$. The column $|\psi_c\rangle$ represents the state complementary to the state of interest (i.e., the other state of the two level system). The last column $f(\tau)$ and $g(\tau)$ are given in Eq. (30) and Eq. (31) respectively.

simply. For example, for $n = 1$, using $|\psi(0)\rangle = |\psi_+\rangle$ and $\hat{Q} = |\psi_c\rangle\langle\psi_c|$ in Eq. (12), we get

$$S_r(1|\tau_1) = \langle\psi_+|e^{iH\tau_1}|\psi_c\rangle\langle\psi_c|e^{-iH\tau_1}|\psi_+\rangle = |\langle\psi_+|e^{iH\tau_1}|\psi_c\rangle|^2. \quad (27)$$

Similarly, from Eq. (15)

$$S_r(2|\tau_1, \tau_2) = |\langle\psi_+|e^{iH\tau_1}|\psi_c\rangle|^2 |\langle\psi_c|e^{iH\tau_2}|\psi_c\rangle|^2. \quad (28)$$

Likewise, for general n in Eq. (17), we have

$$S_r(n|\{\tau_i\}) = |\langle\psi_+|e^{iH\tau_1}|\psi_c\rangle|^2 \prod_{k=2}^n |\langle\psi_c|e^{iH\tau_k}|\psi_c\rangle|^2, \quad (29)$$

where $\{\tau_i\} \equiv \{\tau_1, \tau_2, \dots, \tau_n\}$. For convenience, we define a pair of functions

$$f(\tau) \equiv |\langle\psi_+|e^{iH\tau}|\psi_c\rangle|^2 \quad (30)$$

$$g(\tau) \equiv |\langle\psi_c|e^{iH\tau}|\psi_c\rangle|^2 \quad (31)$$

and their Laplace transforms

$$\int_0^\infty d\tau f(\tau) e^{-s\tau} = \tilde{f}(s), \quad (32)$$

$$\int_0^\infty d\tau g(\tau) e^{-s\tau} = \tilde{g}(s). \quad (33)$$

In terms of the two functions $g(\tau)$ and $f(\tau)$ defined above, Eq. (29) reads

$$S_r(n|\{\tau_i\}) = f(\tau_1) \prod_{k=2}^n g(\tau_k). \quad (34)$$

We next substitute the result in our general formula in Eq. (26). In terms of the Laplace transform in Eq. (33) we get

$$\tilde{S}_r(s) = \frac{1}{r+s} \left[1 + r \tilde{f}(r+s) \sum_{n=1}^{\infty} [r \tilde{g}(r+s)]^{n-1} \right] = \frac{1}{r+s} \left[1 + \frac{r \tilde{f}(r+s)}{1 - r \tilde{g}(r+s)} \right]. \quad (35)$$

This exact Laplace transform requires the knowledge of just two function $f(\tau)$ and $g(\tau)$ defined respectively in Eqs. (30) and (31). Thus, essentially, one needs to just compute two matrix elements $\langle \psi_+ | e^{iH\tau} | \psi_c \rangle$ and $\langle \psi_c | e^{iH\tau} | \psi_c \rangle$. These matrix elements depend, of course, on the details of the two-level Hamiltonian H . But even without computing these matrix elements explicitly, it is possible to extract some general properties of the PDF $F_r(t)$ for a generic two-level Hamiltonian, as demonstrated below.

Probability distribution of the first detection time. We recall from Eq. (5) that $F_r(t) = -dS_r(t)/dt$. Taking Laplace transform with respect to t on both sides and using $S_r(0) = 1$, it follows that

$$\tilde{F}_r(s) = \int_0^\infty F_r(t) e^{-st} dt = 1 - s\tilde{S}_r(s) = 1 - \frac{s}{r+s} \left[\frac{1 + r(\tilde{f}(r+s) - \tilde{g}(r+s))}{1 - r\tilde{g}(r+s)} \right], \quad (36)$$

where we used Eq. (35). This Laplace transform can be formally inverted as

$$F_r(t) = \int_\Gamma \frac{ds}{2\pi i} e^{st} \tilde{F}_r(s). \quad (37)$$

where Γ denotes a Bromwich contour in the complex s space. While inverting this Laplace transform explicitly is hard and it depends on the specific form of $\tilde{g}(s)$, we will see below that some asymptotic behaviors, such as the small t behavior of $F_r(t)$, can be extracted explicitly.

Mean first detection time. The mean first detection time in Eq. (6), upon setting $s = 0$ in Eq. (35), is given by

$$\bar{t}_r = \int_0^\infty t F_r(t) dt = \tilde{S}_r(0) = \frac{1}{r} \left[1 + \frac{r\tilde{f}(r)}{1 - r\tilde{g}(r)} \right]. \quad (38)$$

Below, we analyse $F_r(t)$ and its first moment \bar{t}_r for the two schemes separately.

4.1. First scheme

We start with the first scheme mentioned in Table 1, where $|\psi_{\text{int}}\rangle = |\psi_-\rangle$. Its complementary state is $|\psi_c\rangle = |\psi_+\rangle$. In this case, it follows from Eqs. (30) and (31) that

$$f(\tau) = g(\tau) = |\langle \psi_+ | e^{iH\tau} | \psi_+ \rangle|^2. \quad (39)$$

Hence, from Eq. (33), we have $\tilde{f}(s) = \tilde{g}(s)$. Consequently, Eq. (35) simplifies to

$$\tilde{S}_r(s) = \frac{1}{(r+s)} \frac{1}{[1 - r\tilde{g}(r+s)]}. \quad (40)$$

Using Eq. (36), we get

$$\tilde{F}_r(s) = 1 - s\tilde{S}_r(s) = 1 - \frac{s}{r+s} \left[\frac{1}{1 - r\tilde{g}(r+s)} \right]. \quad (41)$$

Thus we have only one function $\tilde{g}(s)$ that characterizes fully the probability distribution of the first detection time.

Asymptotic behavior of $F_r(t)$ for small and large t . Given a generic $\tilde{g}(s)$, one can then easily deduce the small t behavior of $F_r(t)$ by analysing the large s behavior of $\tilde{F}_r(s)$ in Eq. (41). For this we need to know how $\tilde{g}(s)$ behaves for large s . From Eq. (39) we have, for scheme 1,

$$\tilde{g}(s) = \int_0^\infty d\tau e^{-s\tau} \left| \langle \psi_+ | e^{iH\tau} | \psi_+ \rangle \right|^2. \quad (42)$$

The large s behavior of $\tilde{g}(s)$ is governed by the short time behavior of $g(\tau)$ in Eq. (39). To extract this large s behavior from Eq. (42), it is useful to first make a change of variable $s\tau = \tilde{\tau}$ and rewrite the integral in Eq. (42) as

$$\tilde{g}(s) = \frac{1}{s} \int_0^\infty d\tilde{\tau} e^{-\tilde{\tau}} \left| \langle \psi_+ | e^{iH \frac{\tilde{\tau}}{s}} | \psi_+ \rangle \right|^2. \quad (43)$$

Next we expand $e^{iH \frac{\tilde{\tau}}{s}}$ in a power series of $1/s$ for large s . Keeping terms up to $O(s^{-2})$ we get

$$\tilde{g}(s) = \frac{1}{s} \int_0^\infty d\tilde{\tau} e^{-\tilde{\tau}} \left| \langle \psi_+ | 1 + iH \frac{\tilde{\tau}}{s} - H^2 \frac{\tilde{\tau}^2}{2s^2} + O\left(\frac{\tilde{\tau}^3}{s^3}\right) | \psi_+ \rangle \right|^2. \quad (44)$$

This gives

$$s \tilde{g}(s) = 1 - \frac{2}{s^2} \left[\langle \psi_+ | H^2 | \psi_+ \rangle - \left| \langle \psi_+ | H | \psi_+ \rangle \right|^2 \right] + O(s^{-3}). \quad (45)$$

Therefore, we get

$$\tilde{g}(s) = \frac{1}{s} - \frac{2\sigma^2}{s^3} + \dots \quad (46)$$

where σ^2 is defined as

$$\sigma^2 = \left[\langle \psi_+ | H^2 | \psi_+ \rangle - \left| \langle \psi_+ | H | \psi_+ \rangle \right|^2 \right]. \quad (47)$$

Note that Eq. (46) implies

$$g(\tau) = 1 - \sigma^2 \tau^2 + \dots \quad \text{as } \tau \rightarrow 0. \quad (48)$$

The quantity σ^2 has a nice interpretation: it is the expected variance of the energy in the state $|\psi_+\rangle$. Its expression in Eq. (47) can be further simplified by noting that

$$\begin{aligned} \langle \psi_+ | H^2 | \psi_+ \rangle &= \langle \psi_+ | H \left(|\psi_+\rangle\langle\psi_+| + |\psi_-\rangle\langle\psi_-| \right) H | \psi_+ \rangle \\ &= \left| \langle \psi_+ | H | \psi_+ \rangle \right|^2 + \left| \langle \psi_+ | H | \psi_- \rangle \right|^2. \end{aligned} \quad (49)$$

Substituting Eq. (49) into Eq. (47) gives

$$\sigma^2 = \left| \langle \psi_+ | H | \psi_- \rangle \right|^2. \quad (50)$$

Substituting Eq. (46) into Eq. (41) gives, for large s ,

$$\tilde{F}_r(s) \approx \frac{2r\sigma^2}{s^3}. \quad (51)$$

Consequently, for small t , we obtain the following result for scheme 1, valid for arbitrary two-level system,

$$F_r(t) \approx r\sigma^2 t^2, \quad \text{as } t \rightarrow 0, \quad (52)$$

with σ^2 given in Eq. (50). This early time $\sim t^2$ behavior of $F_r(t)$ emerges from purely quantum dynamics and is universal, i.e., independent of specific measurement protocols [see section (6)].

The large t asymptotic behavior of $F_r(t)$ is more difficult to extract explicitly from its Laplace transform in Eq. (41). However one can easily guess the general form of the asymptotic decay at late times. Depending on $\tilde{g}(s)$, the Laplace transform $\tilde{F}_r(s)$ in Eq. (41) has typically several simple poles in the complex s -plane, all with negative real parts. From Eq. (41), these are given by the roots of $1 - r\tilde{g}(r+s) = 0$. The root whose negative real part is closest to the origin will control the leading late time exponential decay of $F_r(t)$, i.e., we expect $F_r(t) \sim e^{-t/t_m(r)}$ where $1/t_m(r)$ must satisfy $1 - r\tilde{g}(r - 1/t_m(r)) = 0$. In the next section, we demonstrate this computation explicitly in the Jaynes-Cummings model.

Mean first detection time. For the mean first detection time in Eq. (38), one can however extract more detailed information for a generic two level system. For scheme 1, using $\tilde{f}(r) = \tilde{g}(r)$, one gets

$$\bar{t}_r = \frac{1}{r} \frac{1}{[1 - r\tilde{g}(r)]}. \quad (53)$$

One can then compute the asymptotic behaviors of \bar{t}_r for small and large r for any generic two-level system in terms of the small r and large r behaviors of $\tilde{g}(r)$. Using Eq. (46) in Eq. (53), one immediately finds, for large r ,

$$\bar{t}_r \approx \frac{r}{2 \left| \langle \psi_+ | H | \psi_- \rangle \right|^2}, \quad \text{as } r \rightarrow \infty. \quad (54)$$

The fact that the mean detection time diverges as $r \rightarrow \infty$ in scheme 1 can be easily understood as follows. When $r \rightarrow \infty$, the measurement takes place extremely frequently. Consequently, the state of the system essentially does not evolve from its initial state $|\psi_+\rangle$. This is indeed the Zeno limit. So, in scheme 1, the state of interest $|\psi_{\text{int}}\rangle = |\psi_-\rangle$ will never be detected in the large r limit. Naturally, the mean detection time also diverges as $r \rightarrow \infty$ in scheme 1.

To compute the small r behavior of \bar{t}_r we use a different strategy. We again start from the exact expression of $\tilde{g}(r)$ in Eq. (42). We first expand $|\psi_+\rangle$ in the eigenbasis of H and write

$$|\psi_+\rangle = \sum_E a_E |E\rangle, \quad (55)$$

where $|E\rangle$ denotes an eigenvector of H with eigenvalue E . Then the matrix element $\langle\psi_+|e^{iH\tau}|\psi_+\rangle$ can be trivially expressed in this eigenbasis as

$$\langle\psi_+|e^{iH\tau}|\psi_+\rangle = \sum_E |a_E|^2 e^{iE\tau}. \quad (56)$$

Taking the absolute value square gives

$$|\langle\psi_+|e^{iH\tau}|\psi_+\rangle|^2 = \sum_{E,E'} |a_E|^2 |a_{E'}|^2 e^{i(E-E')\tau}. \quad (57)$$

Since the left hand side of Eq. (57) is real, the imaginary part on the right hand side must vanish, leaving

$$|\langle\psi_+|e^{iH\tau}|\psi_+\rangle|^2 = \sum_{E,E'} |a_E|^2 |a_{E'}|^2 \cos((E-E')\tau). \quad (58)$$

We now substitute this exact result [Eq. (58)] in the integral in Eq. (42) and use the identity

$$\int_0^\infty d\tau e^{-r\tau} \cos((E-E')\tau) = \frac{r}{r^2 + (E-E')^2}. \quad (59)$$

This gives us an exact result for $\tilde{g}(r)$, valid for any r ,

$$r \tilde{g}(r) = \sum_{E,E'} |a_E|^2 |a_{E'}|^2 \frac{r^2}{r^2 + (E-E')^2}. \quad (60)$$

We now take the limit $r \rightarrow 0$. In this limit, the ratio

$$\lim_{r \rightarrow 0} \frac{r^2}{r^2 + (E-E')^2} = \delta_{E,E'}, \quad (61)$$

where $\delta_{E,E'}$ is the Kronecker delta function. Then we get from Eq. (60)

$$\lim_{r \rightarrow 0} [r \tilde{g}(r)] = \sum_E |a_E|^4. \quad (62)$$

Substituting this result in Eq. (53) gives, as $r \rightarrow 0$,

$$\bar{t}_r \approx \frac{A_0}{r}, \quad \text{where } A_0 = \frac{1}{\left[1 - \sum_E |a_E|^4\right]}. \quad (63)$$

This result is valid for any two-level Hamiltonian H . The prefactor A_0 can be computed exactly for the Jaynes-Cummings model as we show in the next section (Sec. 5).

Thus, the small and large r behavior of the mean first detection time \bar{t}_r in scheme 1 can be summarized as follows

$$\bar{t}_r \approx \begin{cases} \frac{A_0}{r} & \text{as } r \rightarrow 0, \\ \frac{r}{2|\langle\psi_+|H|\psi_-\rangle|^2} & \text{as } r \rightarrow \infty, \end{cases} \quad (64)$$

with A_0 given in Eq. (63). Thus, \bar{t}_r diverges in the two opposite limits $r \rightarrow 0$ and $r \rightarrow \infty$, provided the amplitude A_0 and the matrix element $\langle \psi_+ | H | \psi_- \rangle$ are both nonzero. In this case, \bar{t}_r is clearly a non-monotonic function of r and typically has a unique minimum at some finite optimal value r^* . This is somewhat reminiscent of the behavior of the mean first passage time to the origin of a Brownian motion on a line, starting at the initial position x_0 and resetting stochastically to x_0 with a constant rate r [4, 5]. However, the latter is a classical system and the physical mechanisms responsible for the emergence of an optimal rate r^* are quite different in quantum and classical systems. Note that in general the amplitude $A_0 > 0$ in Eq. (64) indicating that the divergence A_0/r is quite generic as $r \rightarrow 0$. Hence the condition for the existence of an optimal r^* in scheme 1 translates into the condition that the matrix element $\langle \psi_+ | H | \psi_- \rangle$ is finite. Since this is an off-diagonal element in a two-level system, it is nonzero provided the dynamics induced by the Hamiltonian connects the two states. We will see in the next section (Sec. 5) that in the Jaynes-Cummings model, this dynamics is provided by the nonzero light-matter coupling g that induces the flipping of the spin.

4.2. Second scheme

In the second scheme, we have $|\psi_{\text{int}}\rangle = |\psi_+\rangle$ and hence $|\psi_c\rangle = |\psi_-\rangle$. Using this in Eqs. (30) and (31) gives

$$f(\tau) \equiv |\langle \psi_+ | e^{iH\tau} | \psi_- \rangle|^2, \quad (65)$$

$$g(\tau) \equiv |\langle \psi_- | e^{iH\tau} | \psi_- \rangle|^2. \quad (66)$$

Evidently, $f(\tau) \neq g(\tau)$ and hence $\tilde{f}(s) \neq \tilde{g}(s)$. Consequently, the expression for $\tilde{S}_r(s)$ in Eq. (35) does not simplify further as in the first scheme where $\tilde{f}(s) = \tilde{g}(s)$. However, it turns out that for the second scheme, there exists another identity connecting $\tilde{f}(s)$ and $\tilde{g}(s)$ which reads

$$\tilde{f}(s) + \tilde{g}(s) = \frac{1}{s}. \quad (67)$$

To prove this identity, we add Eq. (65) and Eq. (66) and use the definition $|\psi_+\rangle\langle\psi_+| + |\psi_-\rangle\langle\psi_-| = I$. This gives

$$f(\tau) + g(\tau) = 1. \quad (68)$$

Taking Laplace transform gives Eq. (67). Substituting Eq. (67) in Eq. (35) we get

$$\tilde{S}_r(s) = \frac{1}{(r+s)} \left[2 - \frac{s}{(r+s)(1-r\tilde{g}(r+s))} \right]. \quad (69)$$

Consequently,

$$\tilde{F}_r(s) = 1 - s\tilde{S}_r(s) = 1 - \frac{2s}{(r+s)} - \frac{s^2}{(r+s)^2(1-r\tilde{g}(r+s))}. \quad (70)$$

Asymptotic behavior of $F_r(t)$ for small and large t . As in scheme 1, let us now derive the small t behavior of $F_r(t)$ by analysing the large s behavior of Eq. (70). For scheme 2, $|\psi_c\rangle = |\psi_-\rangle$, and consequently, from Eqs. (31) and (33), we get

$$\tilde{g}(s) = \int_0^\infty d\tau e^{-s\tau} \left| \langle \psi_- | e^{iH\tau} | \psi_- \rangle \right|^2. \quad (71)$$

We then follow exactly the same analysis as in scheme 1 to derive the large s behavior of $\tilde{g}(s)$, just by replacing $|\psi_+\rangle$ in Eq. (42) by $|\psi_-\rangle$. The rest of the analysis goes through and we get exactly the same result as in Eq. (46), where σ^2 happens to be the same as in Eq. (50) since this is invariant under the exchange $|\psi_+\rangle \rightarrow |\psi_-\rangle$. We then substitute Eq. (46) in Eq. (70) and expand for large s . This gives, to leading order, $\tilde{F}_r(s) \approx r/s$ and hence

$$F_r(t) \rightarrow r, \quad \text{as } t \rightarrow 0. \quad (72)$$

Thus, unlike in scheme 1 where $F_r(t)$ vanishes as t^2 as $t \rightarrow 0$ in Eq. (52), in this second scheme $F_r(t)$ approaches a constant r as $t \rightarrow 0$. This drastic difference in the small t behavior in the two schemes can be easily understood as follows. As $t \rightarrow 0$, the system has hardly evolved from its initial state $|\psi_+\rangle$. So, if a measurement takes place (with probability $r dt$ in a small time dt), the state of interest will be definitely detected if it coincides with the initial state $|\psi_+\rangle$ and this is exactly the case in scheme 2. Hence, the probability that a detection occurs in a time interval $[0, dt]$ is simply the probability that a measurement takes place in $[0, dt]$ and this occurs with probability $r dt$. Hence $F_r(t) \rightarrow r$ as $t \rightarrow 0$ in scheme 2. In contrast, in scheme 1, the state of interest $|\psi_-\rangle$ differs from the initial state $|\psi_+\rangle$ and the probability of its detection $[0, dt]$ vanishes as $t \rightarrow 0$.

The large t behavior of $F_r(t)$, as in scheme 1, will be typically exponential and the inverse time scale of the exponential decay is fixed by the pole of $\tilde{F}_r(s)$ in Eq. (70) in the complex s plane. It clearly depends on the details of $\tilde{g}(s)$ and an explicit example will again be worked out in the next section for the Jaynes-Cummings model.

Mean first detection time. The mean first detection time in the second scheme, setting $s = 0$ in Eq. (69), is given by

$$\bar{t}_r = \tilde{S}_r(0) = \frac{2}{r}. \quad (73)$$

This is again strikingly different from the first scheme. In particular, we note that \bar{t}_r in Eq. (73) decays monotonically with increasing r . This is at variance with scheme 1, where \bar{t}_r diverges in both limits $r \rightarrow 0$ and $r \rightarrow \infty$ quite generically, implying the existence of an optimal r^* at an intermediate value. In scheme 2, there is no optimal r^* . The fact that \bar{t}_r vanishes as $r \rightarrow \infty$ limit in scheme 2 can be understood very easily, once again using the implication of the Zeno limit. When $r \rightarrow \infty$, detection attempts take place very frequently and the state stays put in its initial state $|\psi_+\rangle$ at all times. So, in scheme 2 where the state of interest $|\psi_{\text{int}}\rangle$ coincides with the initial state $|\psi_+\rangle$, it will be detected immediately at $t = 0$ (with probability 1) when r is large. Consequently,

the mean detection time must vanish as $r \rightarrow \infty$ in scheme 2, in contrast to scheme 1 where it diverges as $r \rightarrow \infty$. This result in Eq. (73) already appeared in Refs. [56, 57] using a different method, and the ‘topological’ significance of the factor ‘2’ in Eq. (73) was pointed out (see also section (6) for a discussion of this prefactor).

The results presented in this section hold for a general Hamiltonian that is characterized by two levels. Next, in Sec. 5, we will derive explicitly the full first detection probability $F_r(t)$ and the mean detection time \bar{t}_r in a specific two-level system. This is the Jaynes-Cummings Hamiltonian which plays a fundamental role in hybrid quantum systems.

5. Explicit first detection probability in the Jaynes-Cummings model

In this section, we derive explicit results for $F_r(t)$ and its moments for both schemes in the Jaynes-Cummings (JC) model [60–63]. We start by recalling briefly this model.

In the JC model a single spin 1/2 or a qubit (matter) is coupled to a single cavity mode (light) via the Hamiltonian

$$H = \omega_q S^z + \omega_c a^\dagger a + g [S^+ a + a^\dagger S^-], \quad (74)$$

where ω_q is the qubit frequency, ω_c is the cavity frequency and g is the light-matter coupling. Here a/a^\dagger are annihilation/creation operators of bosons and S^\pm, S^z are the Pauli spin operators. The model [Eq. (74)] is defined on a direct product of two spaces, i.e., a two level Hilbert space (spanned by $|\uparrow\rangle, |\downarrow\rangle$) and a single mode cavity Hilbert space (spanned by $|n\rangle$ where $n = 0, 1, 2, 3 \dots$). One can define an excitation operator $\hat{N} = a^\dagger a + S^+ S^-$ which commutes with the Hamiltonian H . For a given excitation sector labelled by n , the Hilbert space is spanned by only two states $|\downarrow, n\rangle$ and $|\uparrow, n-1\rangle$. Since $\hat{N} |\downarrow, n\rangle = n |\downarrow, n\rangle$ and $\hat{N} |\uparrow, n-1\rangle = n |\uparrow, n-1\rangle$, both these states have the same total excitation n and the Hamiltonian does not couple spaces spanned by different excitation sectors. Therefore, given a fixed excitation sector labelled by n , we have effectively a two level system consisting of two states $|\downarrow, n\rangle$ and $|\uparrow, n-1\rangle$. This makes the JC Hamiltonian a putative platform for investigating the probability distribution of the first detection time in a two level system.

The general notation $|\psi_+\rangle$ and $|\psi_-\rangle$ given in Table. 1 and discussed in Sec. 4 now stand for $|\uparrow, n-1\rangle$ and $|\downarrow, n\rangle$ respectively. For the sake of completeness, a detailed description of the JC Hamiltonian and its exact solvability structure is discussed in Appendix A. We will now present results for both schemes represented in Table 1. For the simplicity of presentation, we restrict ourselves to the resonant limit where $\omega_q = \omega_c$. The case $\omega_q \neq \omega_c$ can also be treated, though the results are cumbersome and not illuminating. Hence we restrict ourselves to $\omega_q = \omega_c$ where the formulae become simpler.

5.1. First scheme for the JC Hamiltonian:

We start the system from the initial state

$$|\psi(0)\rangle = |\psi_+\rangle = |\uparrow, n-1\rangle, \quad (75)$$

and recall that in this scheme, the state of interest (detection) is different from the initial state, i.e.,

$$|\psi_{\text{int}}\rangle = |\psi_-\rangle = |\downarrow, n\rangle. \quad (76)$$

Consequently, $|\psi_c\rangle = |\psi_+\rangle = |\uparrow, n-1\rangle$.

To compute the Laplace transform of $F_r(t)$ given in Eq. (41), we need to first compute $\tilde{g}(r+s)$. This can be done explicitly for the JC model, as illustrated below. In order to compute $\tilde{g}(s)$ in Eq. (42), we need to evaluate $e^{iH\tau}|\psi_+\rangle = e^{iH\tau}|\uparrow, n-1\rangle$. In Appendix A.2 we evaluate this and obtain

$$e^{iH\tau}|\psi_+\rangle = e^{iH\tau}|\uparrow, n-1\rangle = e^{i\omega_c(n-1/2)\tau} \left[-i \sin(g\sqrt{n}\tau) |\downarrow, n\rangle + \cos(g\sqrt{n}\tau) |\uparrow, n-1\rangle \right]. \quad (77)$$

It then follows that

$$\left| \langle n-1, \uparrow | e^{iH\tau} |\uparrow, n-1\rangle \right|^2 = \cos^2(g\sqrt{n}\tau). \quad (78)$$

Substituting this result in Eq. (42) gives

$$\tilde{g}(s) = \int_0^\infty d\tau e^{-s\tau} \left| \langle n-1, \uparrow | e^{iH\tau} |\uparrow, n-1\rangle \right|^2 = \frac{1}{s} \frac{2g^2n + s^2}{4g^2n + s^2} \quad (79)$$

Subsequently, from Eqs. (40) and (41), we get

$$\tilde{S}_r(s) = \frac{(r+s)^2 + 4g^2n}{s(r+s)^2 + 2g^2nr + 4g^2ns}, \quad (80)$$

and

$$\tilde{F}_r(s) = \frac{2g^2nr}{s(r+s)^2 + 2g^2nr + 4g^2ns}. \quad (81)$$

Inverting the Laplace transform in Eq. (81) we get

$$F_r(t) = \int_\Gamma \frac{ds}{2\pi i} e^{st} \left[\frac{2g^2nr}{s(r+s)^2 + 2g^2nr + 4g^2ns} \right], \quad (82)$$

where Γ denotes a Bromwich contour in the complex s plane. It turns out to be convenient to rescale $s = r\lambda$ and define the dimensionless parameter

$$\mu = \frac{2g^2n}{r^2}. \quad (83)$$

Upon this rescaling in Eq. (82), one finds that $F_r(t)$ can be expressed in the scaling form

$$F_r(t) = r G_\mu^{(1)}(rt), \quad (84)$$

with

$$G_\mu^{(1)}(z) = \int_\Gamma \frac{d\lambda}{2\pi i} e^{\lambda z} \left[\frac{\mu}{\lambda^3 + 2\lambda^2 + \lambda(1 + 2\mu) + \mu} \right], \quad (85)$$

and the superscript (1) stands for scheme 1. The integrand has three poles ($\lambda_1, \lambda_2, \lambda_3$) in the complex λ plane, all with negative real parts. These are the three roots of the cubic equation

$$\lambda^3 + 2\lambda^2 + \lambda(1 + 2\mu) + \mu = 0, \quad (86)$$

and can be explicitly expressed as

$$\lambda_k = -\frac{1}{3} \left(2 + \zeta^k C + \frac{B_0}{\zeta^k C} \right) \quad \text{for } k = 1, 2, 3 \quad (87)$$

where

$$\zeta = \frac{-1 + i\sqrt{3}}{2}, \quad B_0 = 1 - 6\mu, \quad C = \sqrt[3]{\frac{B_1 + \sqrt{B_1^2 - 4B_0^3}}{2}}, \quad B_1 = -2 - 9\mu. \quad (88)$$

The real parts of all three roots in Eq. (87) are negative. Out of the three roots, λ_1 is real negative and the other two are complex conjugate pairs ($\lambda_3 = \lambda_2^*$) with their common real part smaller than λ_1 . The Bromwich integral in Eq. (85) can then be performed explicitly and is given by the sum of the residues at these three poles. One gets

$$G_\mu^{(1)}(z) = \mu \left[\frac{e^{\lambda_1 z}}{(\lambda_1 - \lambda_2)(\lambda_1 - \lambda_3)} + \frac{e^{\lambda_2 z}}{(\lambda_2 - \lambda_1)(\lambda_2 - \lambda_3)} + \frac{e^{\lambda_3 z}}{(\lambda_3 - \lambda_1)(\lambda_3 - \lambda_2)} \right]. \quad (89)$$

Using $\lambda_3 = \lambda_2^*$, one can further simplify Eq. (89) and express the scaling function $G_\mu^{(1)}(z)$ in terms of only real variables. Defining $\lambda_2 = \lambda_R + i\lambda_I$ and $\lambda_3 = \lambda_R - i\lambda_I$, where $\lambda_R < \lambda_1 < 0$ and $\lambda_I > 0$ are real, we get from Eq. (89)

$$G_\mu^{(1)}(z) = \mu \left[\frac{e^{\lambda_1 z}}{(\lambda_1 - \lambda_R)^2 + \lambda_I^2} - \frac{e^{\lambda_R z} ((\lambda_1 - \lambda_R) \sin(\lambda_I z) + \lambda_I \cos(\lambda_I z))}{\lambda_I ((\lambda_1 - \lambda_R)^2 + \lambda_I^2)} \right]. \quad (90)$$

This result clearly illustrates that $F_r(t) = r G_\mu^{(1)}(rt)$ has two parts: the first part decays purely exponentially $e^{-|\lambda_1|rt}$ at all times, while the second part has oscillatory terms of period $2\pi/r\lambda_I$, but the amplitude of the oscillations dies out exponentially as $e^{-|\lambda_R|rt}$. From this explicit formula, we see that there are three time scales associated with the temporal evolution of $F_r(t)$, given respectively by $t_1 = 1/|r\lambda_1|$, $t_2 = 1/|r\lambda_R|$ and $t_3 = 2\pi/r\lambda_I$. Of the three time scales, t_3 is the shortest. Since $|\lambda_R| > |\lambda_1|$, we have $t_2 < t_1$ and hence the late time exponential decay of $F_r(t)$ is solely governed by the largest time scale t_1 . We will remark more on this important time scale later.

From the exact expression of $F_r(t) = r G_\mu^{(1)}(rt)$, one can easily work out its asymptotic behaviors for small and large t . We get

$$F_r(t) \approx \begin{cases} r g^2 n t^2 & \text{as } t \rightarrow 0 \\ \frac{r\mu}{[(\lambda_1 - \lambda_R)^2 + \lambda_I^2]} e^{-|\lambda_1|rt} & \text{as } t \rightarrow \infty, \end{cases} \quad (91)$$

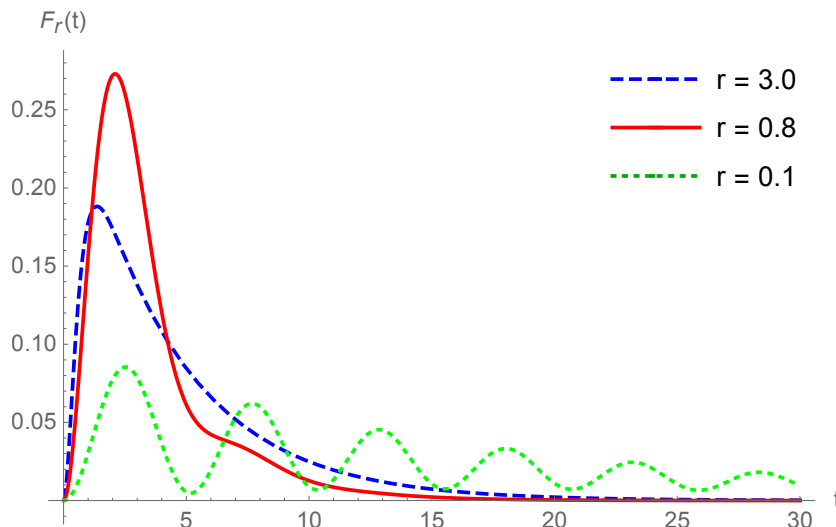


Figure 2. For the first scheme (Table. 1), the PDF $F_r(t)$ in Eq. (84), with $G_\mu^{(1)}(z)$ in Eq. (90), is plotted as a function of t for various values of r . Blue (dashed), red (solid), and green (dotted) correspond to $r = 3.0, 0.8$ and 0.1 respectively. We take light-matter coupling $g = 0.1$ and excitation sector $n = 37$.

where λ_1 , λ_R and λ_I can be read off Eq. (87). We note that the small t behavior in Eq. (91) is in complete agreement with the small t behavior derived in Eq. (52) for a general two level system. This can be verified by computing σ^2 in Eq. (50) for the JC model. We get $\sigma^2 = g^2 n$ (see Eq. (A.6) where the off-diagonal element is precisely σ). In Fig. 2, we plot $F_r(t)$ vs. t for different values of r . One clearly sees oscillations for small values of r , but they get suppressed as r increases. Similarly, for fixed r , the oscillations get suppressed for large t .

The mean first detection time \bar{t}_r , setting $s = 0$ in Eq. (80), reads

$$\bar{t}_r = \tilde{S}_r(0) = \frac{2}{r} + \frac{r}{2g^2 n}. \quad (92)$$

As a function of r , the mean first detection time diverges in the two extreme limits $r \rightarrow 0$ and $r \rightarrow \infty$. One can easily check that the small r behavior $\approx 2/r$ in Eq. (92) matches perfectly with the general small r asymptotics in Eq. (63) valid for arbitrary two-level system. Indeed, for the JC model it is easy to show that $a_E = 1/\sqrt{2}$ for both the energy eigenstates. Hence, in this case, $\sum_E |a_E|^4 = 1/2$. Consequently, from Eq. (63), we get $A_0 = 2$ which is in perfect agreement with the exact result in Eq. (92) as $r \rightarrow 0$. Similarly, the large r behavior $\approx \frac{r}{2g^2 n}$ in Eq. (92) is also consistent with the general large r asymptotic in Eq. (54). To check this, we note that for scheme 1, $|\psi_+\rangle = |\uparrow, n-1\rangle$ and $|\psi_-\rangle = |\downarrow, n\rangle$. The matrix element $\langle \psi_+ | H | \psi_- \rangle$ appearing in Eq. (54) can then be computed for the JC model and is simply given by $g\sqrt{n}$ (see Eq. (A.6) in Appendix A). Consequently, Eq. (54) is fully consistent with the exact large r behavior in Eq. (92).

This non-monotonic dependence of \bar{t}_r on r is structurally similar to the non-

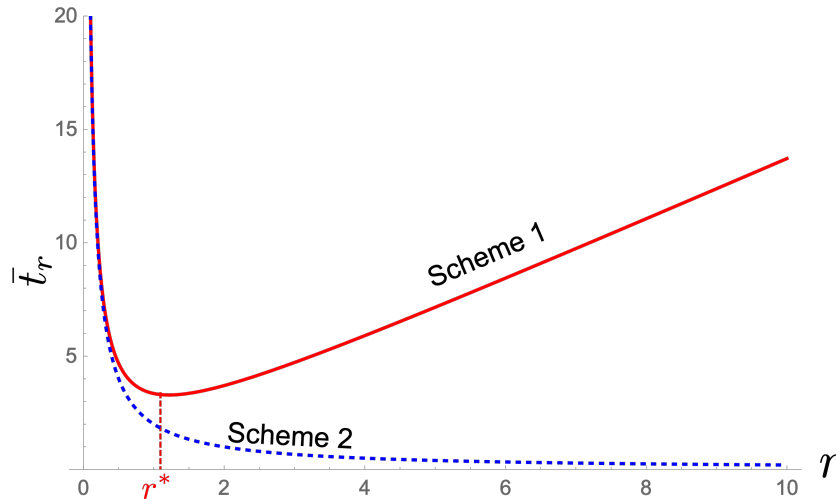


Figure 3. The mean first detection time \bar{t}_r plotted as a function of the measurement rate r , for schemes 1 and 2 [Eq. (92) for scheme 1 and Eq. (107) for scheme 2]. In scheme 1, \bar{t}_r behaves non-monotonically with increasing r with a unique minimum at $r = r^*$, while in scheme 2 it decreases monotonically with increasing r . The location of r^* for scheme 1 [Eq. (93)] is also shown. For scheme 1, we take $g = 0.1$ and $n = 37$. For scheme 2, \bar{t}_r is independent of g and n .

monotonic behavior of the mean first passage time of a classical Brownian motion in the presence of a stochastic resetting with rate r [4, 5]. The mean \bar{t}_r in Eq. (92), as a function of r , has a single unique minimum as $r = r^*$ for which the mean detection time is minimal/optimal. The value of r^* is given by

$$r^* = 2g\sqrt{n}, \quad (93)$$

where we recall that g is the light-matter coupling and n is the label of the fixed excitation sector. At this optimal resetting rate, the value of mean first detection time is

$$\bar{t}_{r=r^*} = \frac{2}{g\sqrt{n}}. \quad (94)$$

In Fig. 3, a plot of \bar{t}_r vs r [Eq. (92)] is shown (red solid line), where the location of the optimal resetting rate [Eq. (93)] is also marked.

Similarly, the second moment is given by

$$\mu_2 = \int_0^\infty F_r(t) t^2 dt = -2\tilde{S}'_r(s=0) = 2\left[\frac{1}{a^2} + \frac{4}{r^2} + \frac{r^2}{4a^4}\right], \quad (95)$$

where $a = g\sqrt{n}$. The variance is given by

$$\sigma_{\text{fd}}^2 = \mu_2 - \mu_1^2 = \frac{4}{r^2} + \frac{r^2}{4a^4}, \quad (96)$$

where the subscript ‘fd’ stands for ‘first detection’. Interestingly, it turns out that the variance in Eq. (96) also has a minimum exactly at the same value of r^* [Eq. (93)], as

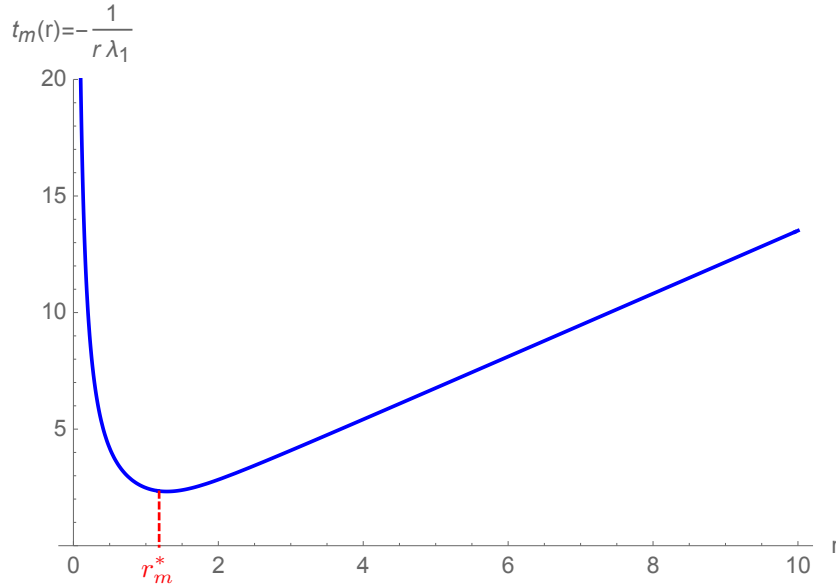


Figure 4. Plot of the maximum waiting time $t_m(r)$ vs. r [Eq. (97)] and also the location of the optimal resetting rate r_m^* . We take $g = 0.1$ and $n = 37$.

for the mean [Eq. (92)]. Thus, not only the mean of the first detection time becomes minimal at $r = r^*$, its fluctuations around the mean are also minimal when $r = r^*$.

Let us conclude this subsection with a final remark. The first moment \bar{t}_r is, by definition, the average amount of time taken for a signal to be detected for the first time. However, the average time may not always be representative of different time scales present in the dynamics. For example, from the exact solution of $F_r(t)$ in Eq. (90), we have seen the existence of three different time scales. In particular, the longest time scale $t_1 = 1/|r \lambda_1|$ governs the decay of $F_r(t)$ at late times [see the second line of Eq. (91)]. The physical meaning of this time scale is as follows: it is clear from Eq. (91) that for $t \gg t_1$, the first detection probability $F_r(t)$ is essentially zero. So, t_1 is effectively the ‘maximal’ time one needs to wait to detect a signal with a nonzero probability. When t exceeds t_1 , the detection probability vanishes almost surely. It is then appropriate to denote this time scale by $t_m(r)$, with the subscript m standing for ‘maximal’, i.e.,

$$t_m(r) = t_1 = -\frac{1}{r \lambda_1}. \quad (97)$$

From the exact expression of λ_1 in Eqs. (87) and (88), one can show that $t_m(r)$ is again a non-monotonic function of r , diverging in the two opposite limits, as

$$t_m(r) \approx \begin{cases} \frac{2}{r} & \text{as } r \rightarrow 0 \\ \frac{r}{2g^2n} & \text{as } r \rightarrow \infty. \end{cases} \quad (98)$$

Thus, interestingly, the asymptotic behaviors of $t_m(r)$ are exactly similar to that of the mean \bar{t}_r in Eq. (92). However, they do differ from each other for intermediate values of r . In Fig. 4, we plot $t_m(r)$ vs. r which also exhibits a unique minimum at some $r = r_m^*$. However, this optimal value differs from the optimal value r^* that minimizes

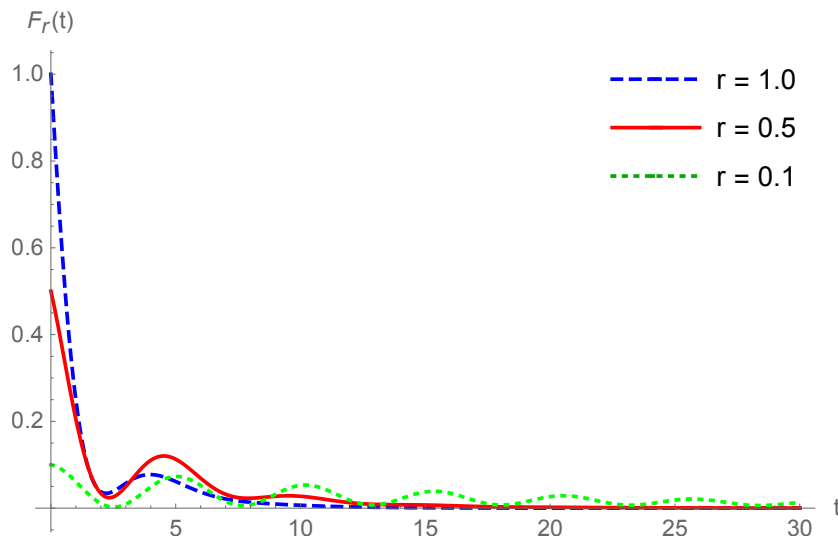


Figure 5. For the second scheme (Table. 1), the distribution of the first detection time $F_r(t)$ [Eq. (103)] is plotted as a function of time t for various values of r . Blue (dashed), red (solid), and green (dotted) correspond to $r = 1.0, 0.5$ and 0.1 respectively. We chose $g = 0.1$ and $n = 37$.

\bar{t}_r . Nevertheless, the fact remains that there is always a certain optimal detection rate r that minimizes the time of detection in scheme 1, no matter which time scale one uses. In the next subsection (Sec. 5.2), we will show that even for scheme 2 where the mean \bar{t}_r decreases monotonically with increasing r , the time scale $t_m(r)$ is identical to that of scheme 1. Hence, choosing $r = r_m^*$ minimizes the maximal detection time scale $t_m(r)$ in both schemes.

5.2. Second scheme for the JC Hamiltonian:

Here again we start the system in the same initial state as in scheme 1 in Eq. (75), but now the state of interest $|\psi_{\text{int}}\rangle$ is given by

$$|\psi_{\text{int}}\rangle = |\psi_+\rangle = |\uparrow, n-1\rangle. \quad (99)$$

Consequently, the complementary state in this case is $|\psi_c\rangle = |\psi_-\rangle = |\downarrow, n\rangle$. Again, to compute the Laplace transform of $F_r(t)$ in Eq. (70), we need to compute $\tilde{g}(s)$ in Eq. (71). The matrix element $\langle \downarrow, n | e^{iH\tau} | \downarrow, n \rangle$ can again be easily evaluated (see Appendix A) and one finds that

$$\tilde{g}(s) = \int_0^\infty d\tau e^{-s\tau} |\langle \downarrow, n | e^{iH\tau} | \downarrow, n \rangle|^2 = \frac{1}{s} \frac{2g^2n + s^2}{4g^2n + s^2}. \quad (100)$$

Consequently, from Eqs. (69) and (70), we get

$$\tilde{S}_r(s) = \frac{4g^2n + s(r+s)}{2g^2n(r+2s) + s(r+s)^2}, \quad (101)$$

and

$$\tilde{F}_r(s) = \frac{r(2g^2n + s(r+s))}{2g^2n(r+2s) + s(r+s)^2}. \quad (102)$$

We next follow the same steps as in Sec. 5.1 including the same change of variables. We get,

$$F_r(t) = r G_\mu^{(2)}(rt), \quad (103)$$

where

$$G_\mu^{(2)}(z) = \int_{\Gamma} \frac{d\lambda}{2\pi i} e^{\lambda z} \left[\frac{\mu + \lambda(\lambda + 1)}{\lambda^3 + 2\lambda^2 + \lambda(1 + 2\mu) + \mu} \right]. \quad (104)$$

Note that the integrand in Eq. (104) has the identical three poles λ_1 , λ_2 and λ_3 as in Sec. 5.1. Evaluating the residues at these poles, one gets

$$G_\mu^{(2)}(z) = \frac{(\mu + \lambda_1(\lambda_1 + 1))e^{\lambda_1 z}}{(\lambda_1 - \lambda_2)(\lambda_1 - \lambda_3)} + \frac{(\mu + \lambda_2(\lambda_2 + 1))e^{\lambda_2 z}}{(\lambda_2 - \lambda_1)(\lambda_2 - \lambda_3)} + \frac{(\mu + \lambda_3(\lambda_3 + 1))e^{\lambda_3 z}}{(\lambda_3 - \lambda_1)(\lambda_3 - \lambda_2)}, \quad (105)$$

where λ_1 , λ_2 and λ_3 are the roots of the cubic equation [Eq. (86)]. As in Sec. 5.1, one can express the scaling function in terms of the real variables λ_1 , λ_R and λ_I which makes the oscillations manifest. But the expression is a bit long and cumbersome, so we omit it here. From the exact result for $F_r(t)$ in scheme 2, one can easily extract its asymptotic behaviors for small and large t , with r fixed. One finds

$$F_r(t) \approx \begin{cases} r & \text{as } t \rightarrow 0 \\ A_2 e^{-|\lambda_1|rt} & \text{as } t \rightarrow \infty, \end{cases} \quad (106)$$

where the amplitude A_2 can be computed in terms of the three roots λ_k 's. We plot $F_r(t) = r G_\mu^{(2)}(rt)$ as a function of t for different values of r in Fig. 5. Note that $F_r(t)$ in the second scheme is drastically different from that in the first scheme (Sec. 5.1), especially at small times t . From Eq. (103), it is easy to see that $F_r(0) = r$ (i.e., a constant). This is also evident in the large- s behaviour for Eq. (102) which gives $\tilde{F}_r(s) \approx r/s$ as $s \rightarrow \infty$. In Fig. (6), we compare $F_r(t)$ vs. t in the two schemes.

Setting $s = 0$ in Eq. (101), the mean detection time for the second scheme becomes

$$\bar{t}_r = \tilde{S}_r(0) = \frac{2}{r} \quad (107)$$

This result shows for the second scheme, there is no finite optimal resetting rate r^* at which the mean first detection time is minimum. In other words, r^* is trivially ∞ . This is quite different from the behavior of \bar{t}_r in scheme 1 which does have a minimum at a finite r^* . In Fig. 3, we show the mean first detection time [Eq. (107)] for the second scheme (blue dotted line), where it is compared to that of the scheme 1 (red solid line).

While the mean detection time is very different in the two schemes, we see that the maximal time scale $t_m(r)$ in scheme 2 is identical to that of scheme 1, and is given by Eq. (97), since the same λ_1 again controls the long time decay of $F_r(t)$ in scheme 2 [see the second line of Eq. (106)]. Consequently, both schemes share the same r_m^* that minimizes the time scale $t_m(r)$.

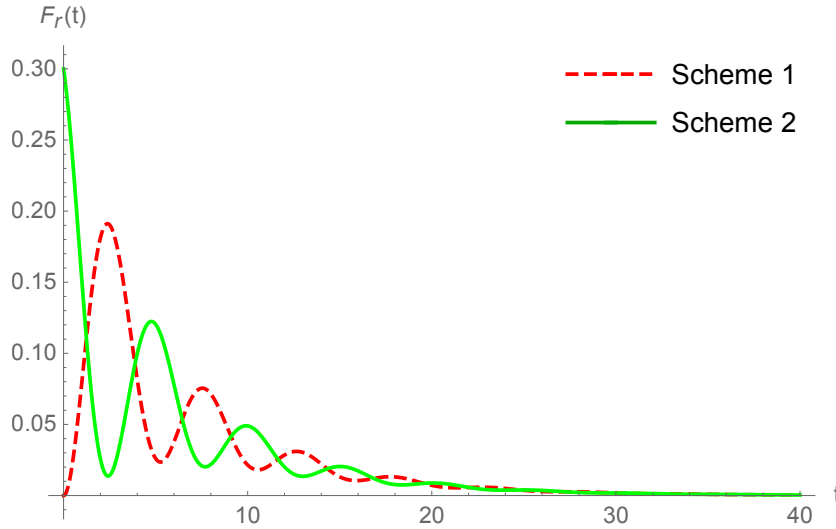


Figure 6. The PDF of the first detection time $F_r(t)$ plotted as a function of t for scheme 1 [Eq. (84)] and scheme 2 [Eq. (103)]. We chose $r = 0.3, g = 0.1$ and $n = 37$.

6. Generalizations to non-Poissonian measurement protocols with a renewal structure

So far in this paper we have focused on Poissonian measurement protocol where in a small time dt , a measurement occurs with probability $r dt$, while with the complementary probability $(1 - r dt)$ no measurement occurs. As mentioned before, this measurement process is Markovian since the probability of a measurement taking place at time t does not depend on the previous history of the measurement. In other words, the measurement process is memoryless. In this case, the intervals between measurements are independent and identically distributed (IID) variables each drawn from $p(\tau) = r e^{-r\tau}$. The framework developed in this paper for this Poissonian measurement protocol can be easily generalised to the case where the measurement events are still uncorrelated as in the Poissonian case, but the waiting time between two successive measurements is distributed via an arbitrary distribution $p(\tau)$, not necessarily exponential. In this case the intervals between measurements are still IID variables, but with a general distribution $p(\tau)$. This is similar to the framework of the continuous-time random walk model. Such a renewal process with arbitrary $p(\tau)$ can not be generated by a memoryless measurement process as in the Poissonian case and in this sense it is sometimes referred to as ‘non-Markovian’, even though the process still has a renewal structure. Only when $p(\tau) = r e^{-r\tau}$ is a pure exponential, the associated renewal process can be realized by a memoryless Markov measurement process. In this section, we show how to compute the PDF $F_r(t)$ of the first detection time for such a non-Poissonian (and non-Markovian) measurement process characterized by IID intervals each drawn from a normalized PDF $p(\tau)$. This generalisation to non-Poissonian waiting time between measurements appeared in Ref. [56] and several results are known, in particular for the return problem, i.e., scheme 2 in our notation. We will see below that the survival probability formalism

developed in this paper also generalizes quite easily and naturally to non-Poissonian case for both schemes 1 and 2.

For a general $p(\tau)$, the probability that there is no measurement in a time interval of duration τ is simply given by

$$q(\tau) = \int_{\tau}^{\infty} p(\tau) d\tau. \quad (108)$$

This follows from the fact that for an interval after a measurement event to remain measurement free up to time τ , the next measurement must occur after time τ , leading to Eq. (108). For the standard Poissonian case, using $p(\tau) = r e^{-r\tau}$, one gets from Eq. (108) $q(\tau) = e^{-r\tau}$, as discussed in earlier sections.

Our general formula for the survival probability $S_r(t)$ in Eq. (18) still holds for a general $p(\tau)$ not necessarily exponential, except that the joint distribution $P(n, \{\tau_i\}|t)$ now has a different expression. Using the IID property of the intervals, we can express it as

$$P(n, \{\tau_i\}|t) = \left[\prod_{k=1}^n p(\tau_k) \right] q\left(t - \sum_{k=1}^n \tau_k\right), \quad (109)$$

which replaces Eq. (19) valid for $p(\tau) = r e^{-r\tau}$. Using again the delta function representation, Eq. (109) can be written in a more convenient form

$$P(n, \{\tau_i\}|t) = \int_0^{\infty} d\tau_{\text{last}} \left[\prod_{k=1}^n p(\tau_k) \right] q(\tau_{\text{last}}) \delta(\tau_1 + \tau_2 + \dots + \tau_n + \tau_{\text{last}} - t). \quad (110)$$

This is the replacement of Eq. (20). Taking Laplace transform with respect to t and integrating over τ_{last} replaces Eq. (21) by

$$\int_0^{\infty} P(n, \{\tau_i\}|t) e^{-st} dt = \tilde{q}(s) \left[\prod_{k=1}^n p(\tau_k) e^{-s\tau_k} \right], \quad (111)$$

where we have defined

$$\tilde{q}(s) = \int_0^{\infty} q(\tau) e^{-s\tau} d\tau. \quad (112)$$

Note that from Eq. (108), it follows that $dq(\tau)/d\tau = -p(\tau)$. Taking Laplace transform and using $q(0) = 1$, one gets

$$\tilde{q}(s) = \frac{1 - \tilde{p}(s)}{s}, \quad (113)$$

where

$$\tilde{p}(s) = \int_0^{\infty} p(\tau) e^{-s\tau} d\tau. \quad (114)$$

One can also check the normalization of the joint PDF $P(n, \{\tau_i\}|t)$. By integrating over τ_i 's in Eq. (111), one gets

$$\int_0^{\infty} P(n|t) e^{-st} dt = \tilde{q}(s) [\tilde{p}(s)]^n. \quad (115)$$

By summing over $n = 0, 1, 2, \dots$, and using the relation in Eq. (113), one easily checks that

$$\int_0^\infty \sum_{n=0}^\infty P(n|t) e^{-st} dt = \frac{1}{s}, \quad (116)$$

implying that $\sum_0^\infty P(n|t) = 1$ for all t .

Substituting Eq. (110) into the general formula [Eq. (18)] and taking Laplace transform with respect to t , we arrive at the expression

$$\tilde{S}_r(s) = \int_0^\infty dt e^{-st} S_r(t) = \tilde{q}(s) + \tilde{q}(s) \sum_{n=1}^\infty \left[\prod_{k=1}^n \int_0^\infty d\tau_k p(\tau_k) e^{-s\tau_k} S_r(n|\{\tau_i\}) \right]. \quad (117)$$

This replaces the result in Eq. (26) valid for $p(\tau) = r e^{-r\tau}$. Note that, as in Eq. (26), we have separated out the $n = 0$ term from the sum.

The result in Eq. (117) is valid for general Hamiltonian and arbitrary $p(\tau)$. To make further progress, we focus on a generic two level system, as in Sec. 4. Since $S_r(n|\{\tau_i\})$ does not depend on $p(\tau)$, it is given by the same expression as in Eq. (34), namely

$$S_r(n|\{\tau_i\}) = f(\tau_1) \prod_{k=2}^n g(\tau_k). \quad (118)$$

where the pair of functions $f(\tau)$ and $g(\tau)$ are still given by Eqs. (30) and (31) respectively. Substituting Eq. (118) in the general result in Eq. (117) and performing the geometric sum over $n = 1, 2, \dots$, we get the exact Laplace transform of the survival probability

$$\tilde{S}_r(s) = \tilde{q}(s) \left[1 + \frac{\tilde{U}(s)}{1 - \tilde{V}(s)} \right], \quad (119)$$

where we have defined

$$\tilde{U}(s) = \int_0^\infty d\tau p(\tau) f(\tau) e^{-s\tau} \quad (120)$$

$$\tilde{V}(s) = \int_0^\infty d\tau p(\tau) g(\tau) e^{-s\tau}. \quad (121)$$

Note that for the exponential case $p(\tau) = r e^{-r\tau}$, we have $\tilde{U}(s) = \tilde{f}(r + s)$ and $\tilde{V}(s) = \tilde{g}(r + s)$ and hence Eq. (119) reduces to Eq. (35). The Laplace transform of the first detection probability is then given by

$$\tilde{F}_r(s) = 1 - s \tilde{S}_r(s) = 1 - s \tilde{q}(s) \left[1 + \frac{\tilde{U}(s)}{1 - \tilde{V}(s)} \right] = 1 - [1 - \tilde{p}(s)] \left[1 + \frac{\tilde{U}(s)}{1 - \tilde{V}(s)} \right]. \quad (122)$$

where we replaced $\tilde{q}(s)$ by its expression in Eq. (113). For the Poissonian case $p(\tau) = r e^{-r\tau}$, Eq. (122) reduces to Eq. (36).

From this central expression in Eq. (122) valid for a generic two level system and arbitrary $p(\tau)$, one can carry out exactly similar analysis as in the previous sections to derive the general properties of the first detection probability and its moments. We will skip some of the details here for the sake of brevity, but point out some salient universal features. We consider the two schemes 1 and 2 separately below.

6.1. First scheme

We recall that in this scheme, the state of interest $|\psi_{\text{int}}\rangle = |\psi_{-}\rangle$ differs from the initial state $|\psi_{+}\rangle$. Hence, in this case $f(\tau) = g(\tau)$ and they are given in Eq. (39). Consequently, from Eqs. (120) and (121), we get $\tilde{U}(s) = \tilde{V}(s)$. Plugging this in Eq. (122) gives

$$\tilde{F}_r(s) = \frac{\tilde{p}(s) - \tilde{V}(s)}{1 - \tilde{V}(s)}, \quad (123)$$

where $\tilde{V}(s)$ is given in Eq. (121) in terms of $g(\tau)$. It is hard to invert this Laplace transform explicitly for general $p(\tau)$ and $g(\tau)$. However, one can extract the asymptotic behavior of $F_r(t)$ for small and large t as follows.

Small t behavior of $F_r(t)$. To extract the small t behavior of $F_r(t)$, we consider the large s behavior of its Laplace transform. Consider first the Laplace transform $\tilde{p}(s)$

$$\tilde{p}(s) = \int_0^\infty p(\tau) e^{-s\tau} d\tau = \frac{1}{s} \int_0^\infty d\tilde{\tau} e^{-\tilde{\tau}} p\left(\frac{\tilde{\tau}}{s}\right), \quad (124)$$

where we rescaled $\tau = \tilde{\tau}/s$. Now, for large s , we can expand $p\left(\frac{\tilde{\tau}}{s}\right)$ in a Taylor series, assuming $p(\tau)$ is analytic near $\tau = 0$ and then perform the integral in Eq. (124) term by term. This yields

$$\tilde{p}(s) = \frac{p(0)}{s} + \frac{p'(0)}{s^2} + \frac{p''(0)}{s^3} + O(s^{-4}). \quad (125)$$

Similarly, $\tilde{V}(s)$ in Eq. (121) can be expanded in a power series in $1/s$. Using $g(\tau) = 1 - \sigma^2 \tau^2$ as $\tau \rightarrow 0$ [see Eq. (48)] where σ^2 is given in Eq. (50), we get large s

$$\tilde{V}(s) = \frac{p(0)}{s} + \frac{p'(0)}{s^2} + \frac{(p''(0) - 2\sigma^2)}{s^3} + O(s^{-4}). \quad (126)$$

Substituting Eqs. (125) and (126) in Eq. (123), we get to leading order for large s

$$\tilde{F}_r(s) \approx \frac{2p(0)\sigma^2}{s^3}. \quad (127)$$

This implies that for small t

$$F_r(t) \approx p(0)\sigma^2 t^2, \quad \text{as } t \rightarrow 0. \quad (128)$$

For the Poissonian case, using $p(0) = r$ one recovers the result in Eq. (52). Thus, as long as $p(0) \neq 0$, one finds that the PDF of the first detection probability exhibits a universal t^2 law for small t , independent of the details of $p(\tau)$ and also of the Hamiltonian of the two level system. The dependence on $p(\tau)$ and on H appears only through the amplitude of this t^2 law, but the behavior $\sim t^2$ is universal as long as $p(0) > 0$. This universal t^2 law emerges from purely quantum dynamics that dominates at early times.

Large t behavior of $F_r(t)$. Extraction of the large t behavior of $F_r(t)$ from its Laplace transform in Eq. (124) is more tricky. If $p(\tau)$ decays exponentially or faster, one needs to investigate the poles of $\tilde{F}_r(s)$ in the complex plane and in that case $F_r(t)$, for large t , will decay exponentially, as was shown in the previous section for the Poissonian protocol. However, if $p(\tau)$ has a power law tail for large τ , e.g.,

$$p(\tau) \approx \frac{A}{\tau^{\mu+1}}, \quad \text{with } \mu > 0, \quad (129)$$

its effect shows up as a singular term in the small s expansion of the Laplace transform $\tilde{F}_r(s)$. Consequently, one can extract the large t behavior of $F_r(t)$ from the singular small s behavior of its Laplace transform. In fact, if $p(\tau)$ has a power law tail as in Eq. (129) for large τ , its Laplace transform behave for small s as

$$\tilde{p}(s) = 1 + \tilde{p}_{\text{reg}}(s) + \tilde{p}_{\text{sing}}(s) \quad (130)$$

where $\tilde{p}_{\text{reg}}(s)$ represents the regular part of the small s expansion and $\tilde{p}_{\text{sing}}(s)$ is the leading singular term given by

$$\tilde{p}_{\text{sing}}(s) \approx A_1 s^\mu \quad \text{where } A_1 = \Gamma(-\mu) A, \quad (131)$$

valid for all non-integer $\mu > 0$ (for a simple proof see the appendix B of Ref. [69]). In Eq. (131), $\Gamma(x)$ denotes the Gamma function. For integer μ , there will be additional multiplicative logarithm in the singular term [69], but we omit the details here. Note that we have used $\tilde{p}(0) = 1$ since $p(\tau)$ is normalized to unity. Similarly, we can expand $\tilde{V}(s)$ into its regular and leading singular parts for small s

$$\tilde{V}(s) = \tilde{V}(0) + \tilde{V}_{\text{reg}}(s) + \tilde{V}_{\text{sing}}(s), \quad (132)$$

where we will not need the detailed form of $\tilde{V}_{\text{sing}}(s)$ as we will see shortly. Substituting Eqs. (130) and (132) in Eq. (123) and keeping only leading order term for small s , we find that $\tilde{V}_{\text{sing}}(s)$ drops out leaving

$$\tilde{F}_r(s) = 1 + \tilde{F}_{\text{reg}}(s) + \frac{A_1}{1 - \tilde{V}(0)} s^\mu, \quad (133)$$

where $\tilde{F}_{\text{reg}}(s)$ represents the regular part of the small s expansion of $\tilde{F}_r(s)$. From this singular small s behavior in Eq. (133), one can then read off the large t behavior of $F_r(t)$

$$F_r(t) \approx \frac{A}{(1 - \tilde{V}(0))} \frac{1}{t^{\mu+1}}, \quad (134)$$

where A is the amplitude of the power law decay of $p(\tau)$ in Eq. (129). Thus, the large t behavior of $F_r(t)$ is completely governed by the large τ behavior of $p(\tau)$, with the amplitude A renormalized by the factor $1/(1 - \tilde{V}(0))$. The information about the Hamiltonian H is contained only in $\tilde{V}(0) = \int_0^\infty d\tau p(\tau) g(\tau)$ through the function $g(\tau)$.

Thus the quantum Hamiltonian in the two level system only affects the amplitude of the late time algebraic decay of $F_r(t)$ in Eq. (134).

The mean detection time and the higher moments can also be computed easily from the Laplace transform $\tilde{F}_r(s)$ in Eq. (123). For instance, if the first moment $\langle \tau \rangle = \int_0^\infty \tau p(\tau) d\tau$ exists, then the mean detection time is given by the exact expression

$$\bar{t}_r = \frac{\langle \tau \rangle}{1 - \tilde{V}(0)} \quad \text{where} \quad \tilde{V}(0) = \int_0^\infty p(\tau) g(\tau) d\tau. \quad (135)$$

6.2. Second scheme

In this scheme, the state of interest $|\psi_{\text{int}}\rangle = |\psi_+\rangle$ is the same as the initial state $|\psi_+\rangle$. In this case, we have $f(\tau) + g(\tau) = 1$ from Eq. (68) and hence $\tilde{f}(s) + \tilde{g}(s) = 1/s$. Adding Eqs. (120) and (121), we then get

$$\tilde{U}(s) + \tilde{V}(s) = \tilde{p}(s). \quad (136)$$

Eliminating $\tilde{U}(s)$ in Eq. (122) using Eq. (136) gives

$$\tilde{F}_r(s) = 1 - \frac{[1 - \tilde{p}(s)] [1 + \tilde{p}(s) - 2\tilde{V}(s)]}{1 - \tilde{V}(s)}. \quad (137)$$

To extract the small t behavior of $F_r(t)$, we expand $\tilde{F}_r(s)$ for large s as in scheme 1 in the previous subsection. Omitting details, we get

$$\tilde{F}_r(s) \approx \tilde{V}(s) \approx \frac{p(0)}{s}, \quad (138)$$

where we used Eq. (126) for the leading large s expansion of $\tilde{V}(s)$. The result in Eq. (138) implies

$$F_r(t) \approx p(0) \quad \text{as} \quad t \rightarrow 0. \quad (139)$$

Thus this limiting small t behavior is completely independent of the Hamiltonian H and it depends only on $p(0)$, as long as $p(0) > 0$. Note that for the Poissonian case $p(\tau) = r e^{-r\tau}$ we have $p(0) = r$, thus recovering the result in Eq. (72).

The large t behavior of $F_r(t)$ can similarly be inferred from its Laplace transform in Eq. (137) following the same procedure as in scheme 1 discussed in the previous subsection. For the case when $p(\tau) = A/\tau^{\mu+1}$ for large τ , we can again use the small s expansion of $\tilde{p}(s)$ and $\tilde{V}(s)$ given respectively in Eqs. (131) and (132). Substituting them in Eq. (137) gives, for small s ,

$$\tilde{F}_r(s) \approx 1 + \tilde{F}_{\text{reg}}(s) + 2p_{\text{sing}}(s) \approx 1 + \tilde{F}_{\text{reg}}(s) + 2A_1 s^\mu, \quad (140)$$

where $\tilde{F}_{\text{reg}}(s)$ is the regular part of the small s behavior of $\tilde{F}_r(s)$ and we have used the result $\tilde{p}_{\text{sing}}(s) \approx A_1 s^\mu$ from Eq. (131). From the singular small s behavior in Eq. (140), one can then read off the large t behavior of $F_r(t)$

$$F_r(t) \approx \frac{2A}{t^{\mu+1}} \quad \text{as} \quad t \rightarrow \infty. \quad (141)$$

Thus in both schemes, the leading large t behavior of $F_r(t)$ has a universal power law tail with exponent $\mu + 1$ that does not depend on the Hamiltonian H . In scheme 1, the dependence on the Hamiltonian shows up in the amplitude through $\tilde{V}(0)$ in Eq. (134). In contrast, in scheme 2, even the amplitude is independent of H , making the large t tail of $F_r(t)$ completely universal.

The mean detection time in scheme 2 can also be computed explicitly from the Laplace transform $\tilde{F}_r(s)$ in Eq. (137). As long as $\langle \tau \rangle = \int_0^\infty \tau p(\tau) d\tau$ exists, the mean first detection time is given by

$$\bar{t}_r = 2 \langle \tau \rangle. \quad (142)$$

As mentioned earlier, this result in Eq. (142) was derived in Refs. [56,57] using a different method and the factor 2 was shown to be the dimension 2 of the Hilbert space for non-degenerate two level systems. A more general result for N level systems states $\bar{t}_r = N \langle \tau \rangle$ where N is the dimension of the Hilbert space in non-degenerate systems. This general result was first discovered for stroboscopic protocol in Ref. [36], and was subsequently generalised to other random protocols in Ref. [56]. For the stroboscopic protocol, the relation in Eq. (142) has been recently measured experimentally using an IBM quantum computer [58].

7. Conclusions and Outlook

To summarize, in this paper we have studied ‘quantum resetting’ purely via random projective measurements. In our system, ‘restart’ is not implemented by classical resetting of a quantum state, but rather the projective measurements at random times perform the resetting. Our main object of interest is the probability distribution $F_r(t)$ of the first detection time of a specified quantum state of interest. We have presented a general framework to compute $F_r(t)$ for arbitrary measurement protocols. We then focused on the protocol where the measurement events are independent, with the waiting time between successive measurements drawn independently from a general PDF $p(\tau)$. The case $p(\tau) = r e^{-r\tau}$ corresponds to the Poissonian protocol where in a small time dt , a measurement occurs with probability $r dt$ and with the complementary probability $(1 - r dt)$ no measurement occurs. We have shown how our general framework yields exact results for $F_r(t)$ in an arbitrary two level system. It turns out that the result depends crucially on the detection schemes involved. We considered two complementary schemes: (1) where the state of interest coincides with and (2) differs from the initial state. Interestingly, the mean first detection time, as a function of the measurement rate r , exhibits markedly different behaviors in the two schemes. In scheme 1, the PDF $F_r(t)$ vanishes as $t \rightarrow 0$ universally as $F_r(t) \sim t^2$ (independent of $p(\tau)$ as long as $p(0) \neq 0$), while in scheme 2, $F_r(t)$ approaches a constant $p(0)$ as $t \rightarrow 0$. Also, the mean detection time in scheme 1 is a non-monotonic function of r with a single minimum at an optimal value r^* , while in scheme 2 it is a monotonically decreasing function of r , signalling the absence of a finite optimal value. These general

predictions are verified via explicit computation in the Jaynes-Cummings model of light-matter interaction. We also generalised our results to non-Poissonian measurement protocols with a renewal structure where the intervals between successive independent measurements are distributed via a general distribution $p(\tau)$. We showed that the short time behavior of $F_r(t) \sim p(0) t^2$ in scheme 1 is universal and this universality is rooted in purely quantum dynamics that dominates at early times.

In this paper, we derived explicit results for the statistics of the first detection time in two complementary detection schemes for a generic two level system subjected to Poissonian (and non-Poissonian) random measurement protocol. It would be interesting to see if our results, especially for scheme 1, can be extended to systems with more than 2 states that are subjected to these random measurement protocols.

The general framework presented here, for Poissonian and non-Poissonian measurement protocols, may be useful in other quantum measurement problems of current interest. For example, a very interesting area of current research concerns measurement induced phase transitions in quantum systems [70–75]. It would be interesting to explore if the formalism developed in this paper can be extended to study the dynamics of entanglement entropy under repeated measurements using Poissonian/non-Poissonian random protocols.

8. Acknowledgements

We thank Eli Barkai for useful discussions. M. K. would like to acknowledge support from the Project 6004-1 of the Indo-French Centre for the Promotion of Advanced Research (IFCPAR), Ramanujan Fellowship (SB/S2/RJN114/2016), SERB Early Career Research Award (ECR/2018/002085) and SERB Matrix Grant (MTR/2019/001101) from the Science and Engineering Research Board (SERB), Department of Science and Technology, Government of India. M. K. acknowledges support from the Department of Atomic Energy, Government of India, under Project No. RTI4001. M. K. thanks the hospitality of LPENS (Paris), LPTHE (Paris) and LPTMS (Paris-Saclay) during several visits. M. K. acknowledges the support from the Science and Engineering Research Board (SERB, government of India), under the VAJRA faculty scheme (No. VJR/2019/000079). S. N. M. acknowledges the support from the Science and Engineering Research Board (SERB, government of India), under the VAJRA faculty scheme (No. VJR/2017/000110).

Appendix A. Exact solvability and quantum time dynamics of the Jaynes-Cummings Hamiltonian

Appendix A.1. Integrability

In this appendix, for the sake of completeness we briefly review the well known Jaynes-Cummings (JC) Hamiltonian [60–63] and discuss its exact solvability. The Jaynes-

Cummings Hamiltonian is given by

$$H = \omega_q S^z + \omega_c a^\dagger a + g[S^+ a + a^\dagger S^-], \quad (\text{A.1})$$

where ω_q is the qubit frequency, ω_c is the cavity frequency and g is the light-matter coupling. Here a/a^\dagger are annihilation/creation operators of bosons and S^\pm, S^z are the Pauli spin operators. The model [Eq. (A.1)] is defined on a direct product of two spaces, i.e., a two level Hilbert space (spanned by $|\uparrow\rangle, |\downarrow\rangle$) and a single mode cavity Hilbert space (spanned by $|n\rangle$ where $n = 0, 1, 2, 3, \dots$). The algebra for operators is given by

$$[a, a^\dagger] = 1, [S^z, S^\pm] = \pm S^\pm, [S^+, S^-] = 2S^z. \quad (\text{A.2})$$

Let us define an excitation operator \hat{N} as

$$\hat{N} = a^\dagger a + S^+ S^-. \quad (\text{A.3})$$

It is easy to check that [using Eq. (A.2)] the operator \hat{N} and H commute with each other, i.e.,

$$[H, \hat{N}] = 0. \quad (\text{A.4})$$

Also, from Eq. (A.3), one can show

$$\hat{N} |\downarrow, n\rangle = n |\downarrow, n\rangle, \quad \hat{N} |\uparrow, n-1\rangle = n |\uparrow, n-1\rangle. \quad (\text{A.5})$$

From Eq. (A.5), one concludes that for a given excitation sector labelled by n , the Hilbert space is spanned by only two states $|\downarrow, n\rangle$ and $|\uparrow, n-1\rangle$. The Hamiltonian does not couple spaces spanned by different sectors. Therefore, in a given excitation sector labelled by n , the JC Hamiltonian can be represented by a 2×2 matrix

$$\begin{aligned} H_n &= \begin{bmatrix} \langle \downarrow, n | H | \downarrow, n \rangle & \langle \downarrow, n | H | \uparrow, n-1 \rangle \\ \langle \uparrow, n-1 | H | \downarrow, n \rangle & \langle \uparrow, n-1 | H | \uparrow, n-1 \rangle \end{bmatrix} \\ &= \begin{bmatrix} -\frac{\omega_q}{2} + \omega_c n & g\sqrt{n} \\ g\sqrt{n} & \frac{\omega_q}{2} + \omega_c(n-1) \end{bmatrix}. \end{aligned} \quad (\text{A.6})$$

The eigenvectors and eigenvalues of H_n [Eq. (A.6)] are given by

$$\begin{aligned} |n, +\rangle &= \cos(\theta_n) |\downarrow, n\rangle + \sin(\theta_n) |\uparrow, n-1\rangle, \\ |n, -\rangle &= -\sin(\theta_n) |\downarrow, n\rangle + \cos(\theta_n) |\uparrow, n-1\rangle, \end{aligned} \quad (\text{A.7})$$

and

$$E_{n\pm} = \omega_c \left(n - \frac{1}{2} \right) \pm \frac{1}{2} \sqrt{(\omega_c - \omega_q)^2 + 4g^2 n}. \quad (\text{A.8})$$

In Eq. (A.7), θ_n (mixing angle) is defined to be

$$\theta_n = \frac{1}{2} \tan^{-1} \left[\frac{2g\sqrt{n}}{\omega_c - \omega_q} \right]. \quad (\text{A.9})$$

Therefore, in a given sector the JC Hamiltonian [Eq. (A.1)] is exactly solvable (integrable).

Appendix A.2. Initial value problem

After establishing the integrability/exact solvability, we will now discuss the initial value problem, i.e., how a state evolves in time starting from an initial state. Let us choose the following initial condition

$$|\psi(0)\rangle = |\uparrow, n-1\rangle. \quad (\text{A.10})$$

We will now find out how the initial condition in Eq. (A.10) evolves when subjected to the JC Hamiltonian [Eq. (A.1)]. In other words, we need to evaluate

$$|\psi(t)\rangle = e^{-iHt}|\psi(0)\rangle = e^{-iHt} |\uparrow, n-1\rangle. \quad (\text{A.11})$$

To simplify things further, we will stay in the resonant limit, $\omega_c = \omega_q$ which implies $\theta_n = \pi/4$ [Eq. (A.9)]. In this resonant limit, Eq. (A.7) and Eq. (A.8) simplify to

$$\begin{aligned} |n, +\rangle &= \frac{1}{\sqrt{2}} \left[|\uparrow, n-1\rangle + |\downarrow, n\rangle \right], \\ |n, -\rangle &= \frac{1}{\sqrt{2}} \left[|\uparrow, n-1\rangle - |\downarrow, n\rangle \right], \end{aligned} \quad (\text{A.12})$$

and

$$E_{n\pm} = \omega_c \left(n - \frac{1}{2} \right) \pm g\sqrt{n}. \quad (\text{A.13})$$

Inverting Eq. (A.12), we get

$$\begin{aligned} |\uparrow, n-1\rangle &= \frac{1}{\sqrt{2}} \left[|n, +\rangle + |n, -\rangle \right], \\ |\downarrow, n\rangle &= \frac{1}{\sqrt{2}} \left[|n, +\rangle - |n, -\rangle \right]. \end{aligned} \quad (\text{A.14})$$

Using Eq. (A.14), Eq. (A.11) then becomes

$$|\psi(t)\rangle = e^{-iHt} |\uparrow, n-1\rangle = \frac{1}{\sqrt{2}} \left[e^{-iE_{n+}t} |n, +\rangle + e^{-iE_{n-}t} |n, -\rangle \right]. \quad (\text{A.15})$$

Substituting the the expressions for $E_{n\pm}$ from Eq. (A.13) in Eq. (A.15), we get

$$|\psi(t)\rangle = e^{-i\omega_c \left(n - \frac{1}{2} \right) t} \left[-i \sin(g\sqrt{nt}) |\downarrow, n\rangle + \cos(g\sqrt{nt}) |\uparrow, n-1\rangle \right]. \quad (\text{A.16})$$

From Eq. (A.16), we can see that the probability that the system stays in excited state is

$$P_e(t) = \langle \psi(t) | \uparrow \rangle \langle \uparrow | \psi(t) \rangle = \cos^2(g\sqrt{nt}). \quad (\text{A.17})$$

and similarly the probability that the system stays in ground state is given by

$$P_g(t) = \langle \psi(t) | \downarrow \rangle \langle \downarrow | \psi(t) \rangle = \sin^2(g\sqrt{nt}). \quad (\text{A.18})$$

Similar to Eq. (A.15), if we had started with an initial state $|\psi(0)\rangle = |\downarrow, n\rangle$ we get

$$\begin{aligned} |\psi(t)\rangle &= \frac{1}{\sqrt{2}} \left[e^{-iE_{n+}t} |n, +\rangle - e^{-iE_{n-}t} |n, -\rangle \right] \\ &= e^{-i\omega_c \left(n - \frac{1}{2} \right) t} \left[-i \sin(g\sqrt{nt}) |\uparrow, n\rangle + \cos(g\sqrt{nt}) |\downarrow, n-1\rangle \right]. \end{aligned} \quad (\text{A.19})$$

Using similar analysis, one can solve the JC model for any arbitrary initial condition by exploiting the fact that the Hamiltonian takes a block diagonal form consisting of 2×2 sectors. The results presented in this appendix were used in Sec. 5 for computing the first detection probability for the JC system.

References

- [1] M. R. Evans, S. N. Majumdar, and G. Schehr, *Stochastic resetting and applications*, J. Phys. A: Math. Theor. **53**, 193001 (2020).
- [2] S. Gupta, A. M. Jayannavar, *Stochastic Resetting: A (Very) Brief Review*, Aip Conf. Proc. **10**, 130 (2022).
- [3] A. Pal, S. Kostinski, S. Reuveni, *The inspection paradox in stochastic resetting*, J. Phys. A: Math. Theor. **55**, 021001 (2022).
- [4] M. R. Evans and S. N. Majumdar, *Diffusion with Stochastic Resetting*, Phys. Rev. Lett. **106**, 160601 (2011).
- [5] M. R. Evans and S. N. Majumdar, *Diffusion with Optimal Resetting*, J. Phys. A: Math. Theor. **44**, 435001 (2011).
- [6] A. Pal, A. Kundu, M. R. Evans, *Diffusion under time-dependent resetting*, J. Phys. A: Math. Theor. **49**, 225001 (2016).
- [7] S. Reuveni, *Optimal Stochastic Restart Renders Fluctuations in First Passage Times Universal*, Phys. Rev. Lett. **116**, 170601 (2016).
- [8] M. R. Evans, S. N. Majumdar, *Diffusion with resetting in arbitrary spatial dimension*, J. Phys. A: Math. Theor. **47**, 285001 (2014).
- [9] L. Kusmierz, S. N. Majumdar, S. Sabhapandit, G. Schehr, *First Order Transition for the Optimal Search Time of Lévy Flights with Resetting*, Phys. Rev. Lett. **113**, 220602 (2014).
- [10] S. Gupta, S. N. Majumdar, G. Schehr, *Fluctuating interfaces subject to stochastic resetting*, Phys. Rev. Lett. **112**, 220601 (2014).
- [11] S. N. Majumdar, S. Sabhapandit, G. Schehr, *Dynamical transition in the temporal relaxation of stochastic processes under resetting*, Phys. Rev. E **91**, 052131 (2015).
- [12] C. Christou, A. Schadschneider, *Diffusion with resetting in bounded domains*, J. Phys. A: Math. Theor. **48**, 285003 (2015).
- [13] D. Campos, V. Méndez, *Phase transitions in optimal search times: How random walkers should combine resetting and flight scales*, Phys. Rev. E **92**, 062115 (2015).
- [14] M. Montero, J. Villarroel, *Directed random walk with random restarts: The Sisyphus random walk*, Phys. Rev. E **94**, 032132 (2016).
- [15] A. Pal, S. Reuveni, *First Passage under Restart*, Phys. Rev. Lett. **118**, 030603 (2017).
- [16] A. Chechkin, I. M. Sokolov, *Random Search with Resetting: A Unified Renewal Approach*, Phys. Rev. Lett. **121**, 050601 (2018).
- [17] M. Magoni, S. N. Majumdar, G. Schehr, *Ising model with stochastic resetting*, Phys. Rev. Research **2**, 033182 (2020).
- [18] P. C. Bressloff, *Diffusion-mediated surface reactions and stochastic resetting*, J. Phys. A: Math. Theor. **53**, 425001 (2020).
- [19] R. G. Pinsky, *Diffusive search with spatially dependent resetting*, Stoch. Proc. Appl. **130**, 2954 (2020).
- [20] B. De Bruyne, S. N. Majumdar, G. Schehr, *Optimal Resetting Brownian Bridges via Enhanced Fluctuations*, Phys. Rev. Lett. **128**, 200603 (2022).
- [21] M. Biroli, H. Larralde, S. N. Majumdar, and G. Schehr, *Extreme Statistics and Spacing Distribution in a Brownian Gas Correlated by Resetting*, Phys. Rev. Lett. **130**, 207101 (2023).
- [22] M. Biroli, S. N. Majumdar, G. Schehr, *Critical number of walkers for diffusive search processes with resetting*, arXiv preprint: 2303.18012.

- [23] O. Tal-Friedman, A. Pal, A. Sekhon, S. Reuveni, Y. Roichman, *Experimental Realization of Diffusion with Stochastic Resetting*, J. Phys. Chem. Lett. **11**, 7350 (2020).
- [24] B. Besga, A. Bovon, A. Petrosyan, S. N. Majumdar, S. Ciliberto, *Optimal mean first-passage time for a Brownian searcher subjected to resetting: Experimental and theoretical results*, Phys. Rev. Research **2**, 032029(R) (2020).
- [25] F. Faisant, B. Besga, A. Petrosyan, S. Ciliberto, S. N. Majumdar, *Optimal mean first-passage time of a Brownian searcher with resetting in one and two dimensions: experiments, theory and numerical tests*, J. Stat. Mech., 113203 (2021).
- [26] B. Mukherjee, K. Sengupta, and S. N. Majumdar, *Quantum dynamics with stochastic reset*, Phys. Rev. B **98**, 104309 (2018).
- [27] D. C. Rose, H. Touchette, I. Lesanovsky, J. P. Garrahan, *Spectral properties of simple classical and quantum reset processes*, Phys. Rev. E **98**, 022129 (2018).
- [28] G. Peretto, F. Carollo, M. Magoni, and I. Lesanovsky, *Designing nonequilibrium states of quantum matter through stochastic resetting*, Phys. Rev. B **104**, L180302 (2021).
- [29] G Peretto, F. Carollo, I. Lesanovsky, *Thermodynamics of quantum-jump trajectories of open quantum systems subject to stochastic resetting*, SciPost Phys. **13**, 079 (2022).
- [30] H. Wiseman, G. Milburn, *Quantum Measurement and Control* (Cambridge University Press, Cambridge, 2009).
- [31] M. A. Nielsen, I. Chuang, *Quantum computation and quantum information* (Cambridge University Press, Cambridge, 2010).
- [32] K. Jacobs, *Quantum Measurement Theory and its Applications* (Cambridge University Press, Cambridge, 2014).
- [33] H. Krovi and T. A. Brun, *Hitting time for quantum walks on the hypercube*, Phys. Rev. A **73**, 032341 (2006).
- [34] H. Krovi and T. A. Brun, *Quantum walks with infinite hitting times*, Phys. Rev. A **74**, 042334 (2006).
- [35] M. Varbanov, H. Krovi, and T. A. Brun, *Hitting time for the continuous quantum walk*, Phys. Rev. A **78**, 022324 (2008).
- [36] F. A. Grünbaum, L. Velázquez, A. H. Werner, R. F. Werner, *Recurrence for discrete time unitary evolutions*, Commun. Math. Phys. **320**, 543 (2013).
- [37] S. Dhar, S. Dasgupta, A. Dhar, *Quantum time of arrival distribution in a simple lattice model*, J. Phys. A: Math. Theor. **48**, 115304 (2015).
- [38] S. Dhar, S. Dasgupta, A. Dhar, D. Sen, *Detection of a quantum particle on a lattice under repeated projective measurements*, Phys. Rev. A **91**, 062115 (2015).
- [39] H. Friedman, D. A. Kessler, and E. Barkai, *Quantum walks: The first detected passage time problem*, Phys. Rev. E **95**, 032141 (2017).
- [40] F. Thiel, E. Barkai, D. Kessler, *First detected arrival of a quantum walker on an infinite line*, Phys. Rev. Lett. **120**, 040502 (2018).
- [41] R. Yin, K. Ziegler, F. Thiel, E. Barkai, *Large fluctuations of the first detected quantum return time*, Phys. Rev. Research **1**, 033086 (2019).
- [42] S. Lahiri, A. Dhar, *Return to the origin problem for a particle on a one-dimensional lattice with quasi-Zeno dynamics*, Phys. Rev. A **99**, 012101 (2019).
- [43] K. Snizhko, P. Kumar, A. Romito, *Quantum Zeno effect appears in stages*, Phys. Rev. Research **2**, 033512 (2020).
- [44] Q. Liu, R. Yin, K. Ziegler, E. Barkai, *Quantum walks: the mean first detected transition time*, Phys. Rev. Research **2**, 033113 (2020).
- [45] V. Dubey, C. Bernardin, and A. Dhar, *Quantum dynamics under continuous projective measurements: Non-Hermitian description and the continuum-space limit*, Phys. Rev. A **103**, 032221 (2021).
- [46] S. Dattagupta, D. Das, S. Gupta, *Stochastic resets in the context of a tight-binding chain driven by an oscillating field*, J. Stat. Mech. 103210 (2021).

- [47] D. Das, S. Dattagupta, S. Gupta, *Quantum unitary evolution interspersed with repeated non-unitary interactions at random times: the method of stochastic Liouville equation, and two examples of interactions in the context of a tight-binding chain*, J. Stat. Mech. 053101 (2022).
- [48] D. Das, S. Gupta, *Quantum random walk and tight-binding model subject to projective measurements at random times*, J. Stat. Mech.: Theory Exp. 033212 (2022).
- [49] M. Magoni, F. Carrolo, G. Peretto, I. Lesanovsky, *Emergent quantum correlations and collective behavior in noninteracting quantum systems subject to stochastic resetting*, Phys. Rev. A **106**, 052210 (2022).
- [50] V. Dubey, R. Chetrite, A. Dhar, *Quantum resetting in continuous measurement induced dynamics of a qubit*, J. Phys. A: Math. Theor. **56**, 154001 (2023).
- [51] F. J Sevilla, A. Valdés-Hernández, *Dynamics of closed quantum systems under stochastic resetting*, J. Phys. A: Math. Theor. **56** 034001 (2023).
- [52] R. Yin, E. Barkai, *Restart expedites quantum walk hitting times*, Phys. Rev. Lett. **130**, 050802 (2023).
- [53] R. Yin, E. Barkai, *Instability in the quantum restart problem*, arXiv preprint: 2301.06100.
- [54] G. Lami, A. Santini, M. Collura, *Continuously Monitored Quantum Systems Beyond Lindblad Dynamics*, arXiv preprint: 2305.04108.
- [55] F. Thiel, I. Muallem, D. Meidan, E. Barkai, and D. A. Kessler, *Dark states of quantum search cause imperfect detection* Phys. Rev. Research **2**, 043107 (2020).
- [56] D. A. Kessler, E. Barkai, K. Ziegler, *First-detection time of a quantum state under random probing* Phys. Rev. A **103**, 022222 (2021)
- [57] K. Ziegler, E. Barkai, D. Kessler, *Randomly repeated measurements on quantum systems: correlations and topological invariants of the quantum evolution* J. Phys. A: Math. Theor. **54**, 395302 (2021).
- [58] S. Tornow, K. Ziegler, *Measurement induced quantum walks on an IBM Quantum Computer*, arXiv preprint: 2210.09941.
- [59] X. Turkeshi, M. Dalmonte, R. Fazio, and M. Schiro, Phys. Rev. B, *Entanglement transitions from stochastic resetting of non-Hermitian quasiparticles*, **105**, L241114 (2022).
- [60] M. O. Scully and M. S. Zubairy, *Quantum Optics* (Cambridge University Press, Cambridge, 1997).
- [61] H. J. Carmichael, *Statistical Methods in Quantum Optics 1: Master Equations and Fokker-Planck Equations*, Springer Science & Business Media, (1999).
- [62] S. Haroche and J. M. Raimond, *Exploring the Quantum: Atoms, Cavities, and Photons*, (Oxford University Press, Oxford, 2006).
- [63] G. S. Agarwal, *Quantum Optics* (Cambridge University Press, Cambridge, 2013).
- [64] F. Mori, P. Le Doussal, S. N. Majumdar, and G. Schehr, *Universal Survival Probability for a d-Dimensional Run-and-Tumble Particle*, Phys. Rev. Lett., **124**, 090603 (2020).
- [65] F. Mori, P. Le Doussal, S. N. Majumdar, and G. Schehr, *Universal properties of a run-and-tumble particle in arbitrary dimension*, Phys. Rev. E **102**, 042133 (2020).
- [66] N. R. Smith, S. N. Majumdar, *Condensation transition in large deviations of self-similar Gaussian processes with stochastic resetting*, J. Stat. Mech. 053212 (2022).
- [67] N. R. Smith, S. N. Majumdar, and G. Schehr, *Striking universalities in stochastic resetting processes*, arXiv preprint: 2301.11026.
- [68] W. Feller, *An Introduction to Probability Theory and its Applications* (New York: Wiley, 1957).
- [69] M. R. Evans, S. N. Majumdar, R. K. P. Zia, *Canonical analysis of condensation in factorized steady states*, J. Stat. Phys. **123**, 357 (2006) .
- [70] Y. Li, X. Chen, and M. P. A. Fisher, *Measurement-driven entanglement transition in hybrid quantum circuits*, Phys. Rev. B **100**, 134306 (2019) .
- [71] B. Skinner, J. Ruhman, and A. Nahum, *Measurement-Induced Phase Transitions in the Dynamics of Entanglement*, Phys. Rev. X **9**, 031009 (2019).
- [72] M. J. Gullans, D. A. Huse, *Dynamical Purification Phase Transition Induced by Quantum*

Measurements, Phys. Rev. X **10**, 041020 (2020),

- [73] A. Zabalo, M. J. Gullans, J. H. Wilson, S. Gopalakrishnan, D. A. Huse, and J. H. Pixley, *Critical properties of the measurement-induced transition in random quantum circuits*, Phys. Rev. B **101**, 060301 (2020).
- [74] S. Roy, J. T. Chalker, I. V. Gornyi, and Y. Gefen, *Measurement-induced steering of quantum systems*, Phys. Rev. Research **2**, 033347 (2020)
- [75] P. Sierant, M. Schiro, M. Lewenstein, and X. Turkeshi, *Measurement-induced phase transitions in $(d + 1)$ -dimensional stabilizer circuits*, Phys. Rev. B **106**, 214316 (2022).